

Large-scale and Deep Processes

**Thermal-petrologic-fluid flow: structure
and dynamics of subduction zones**

Ikuko Wada – Virginia Tech

in collaboration with

Kelin Wang¹, John He¹, Roy D. Hyndman¹, Mark D. Behn²,
Alison M. Shaw², Catherine A. Rychert³, E. Marc Parmentier⁴

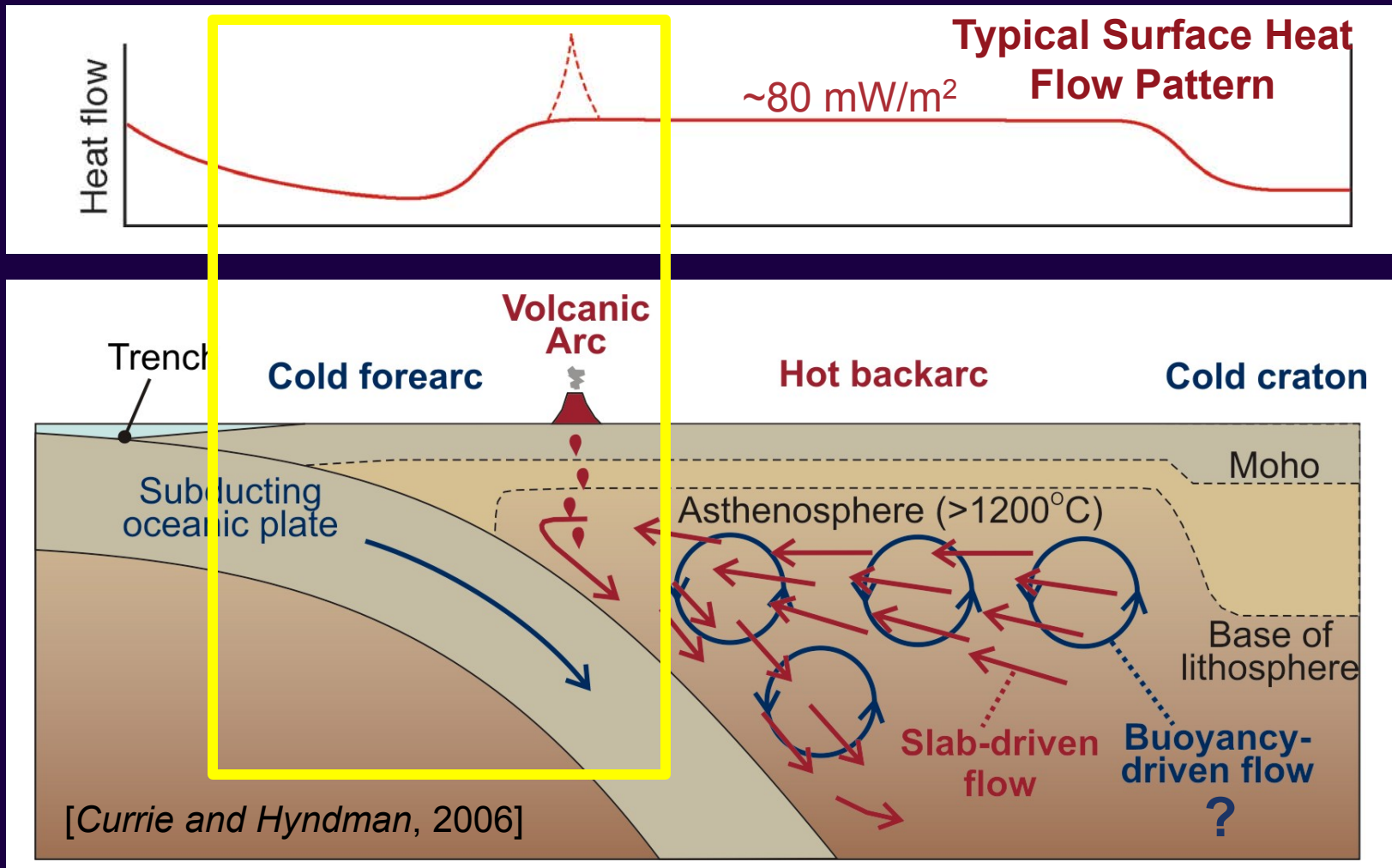
¹ Pacific Geoscience Centre, Geological Survey of Canada

² Woods Hole Oceanographic Institution, MA

³ University of Bristol, UK

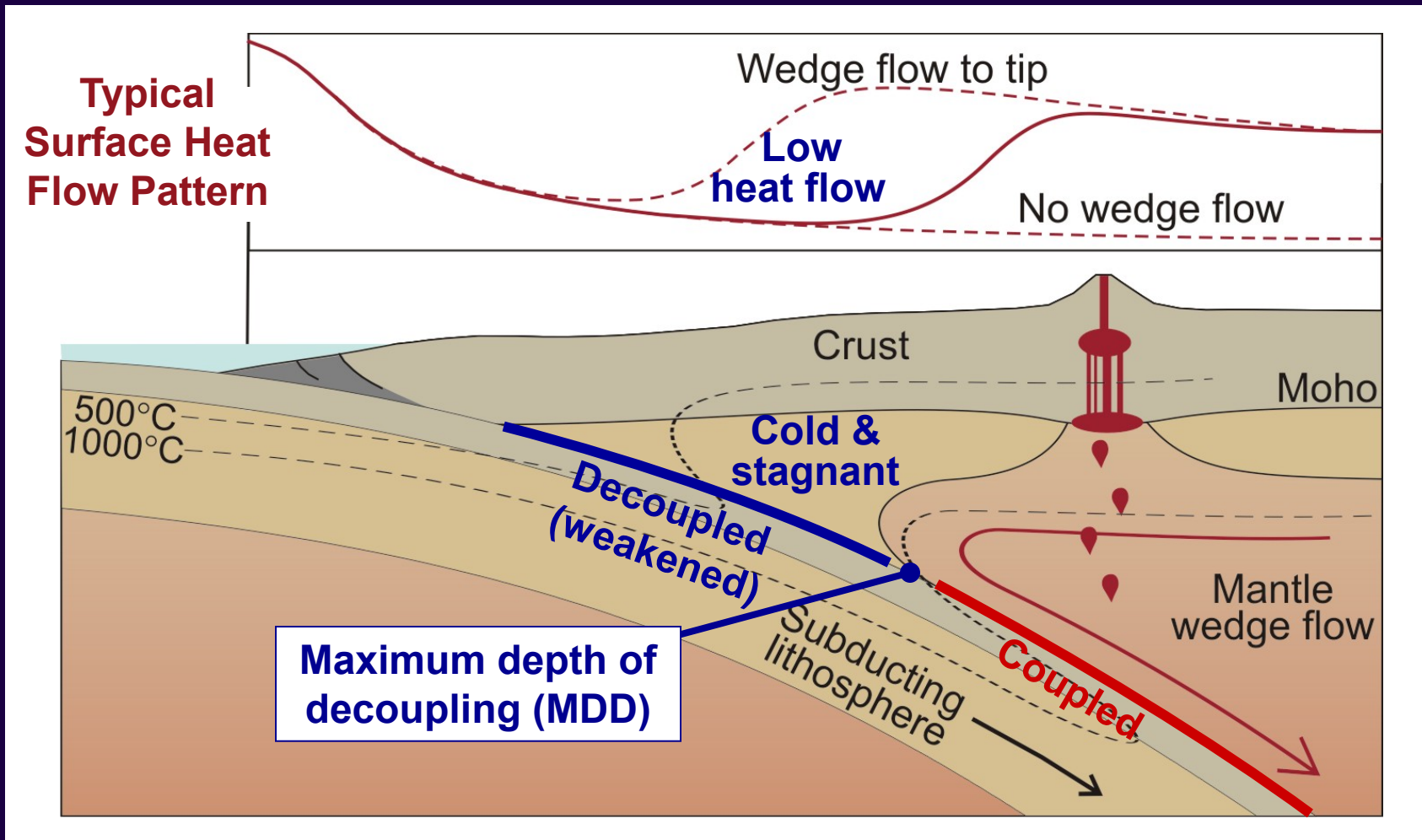
⁴ Brown University, RI

Mantle Flow in Subduction Zones



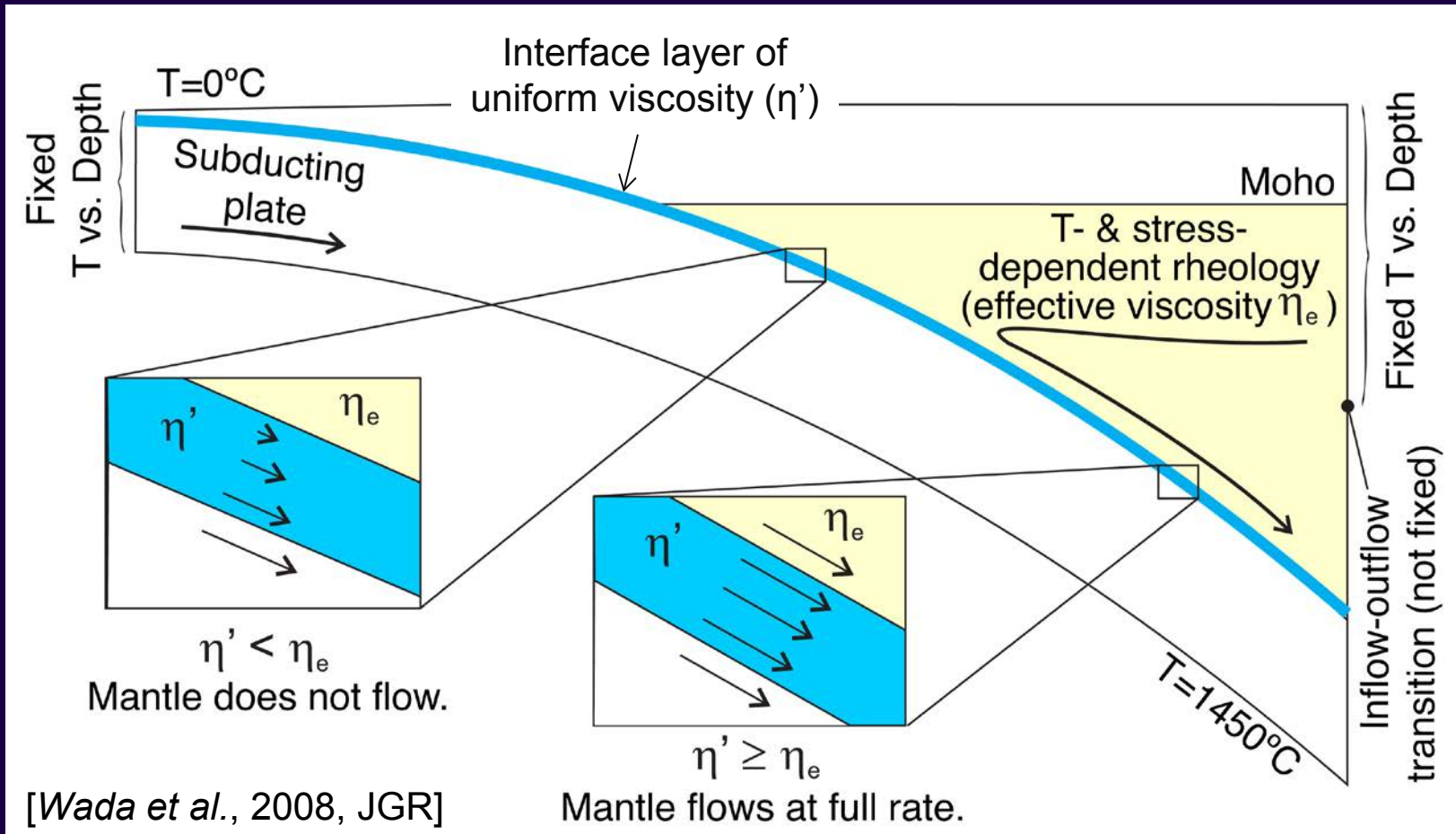
The overall thermal structure depends strongly on the age of the slab and mantle wedge flow.

Mantle Flow beneath the Forearc and Arc



The maximum depth of decoupling (MDD) controls the trenchward extent of mantle wedge flow.

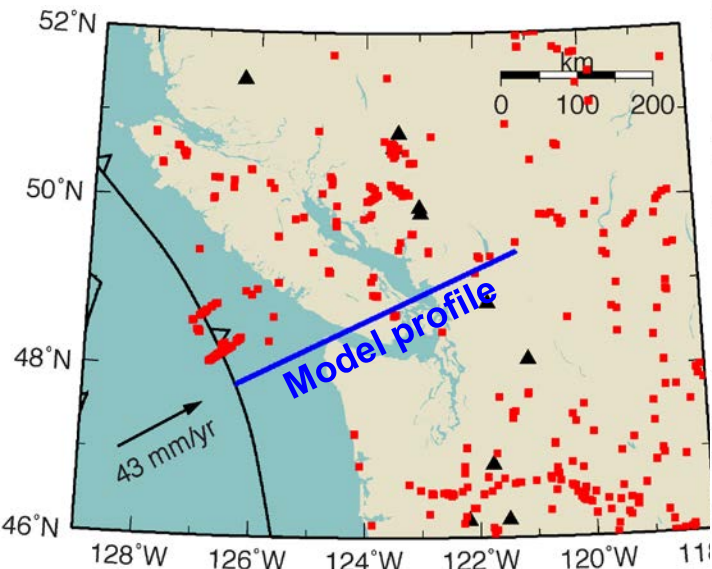
Interface Layer Approach



Decoupling depends on the strength contrast between the interface (η') and the overlying mantle (η_e).

Maximum Depth of Decoupling (MDD) in N. Cascadia

Northern Cascadia

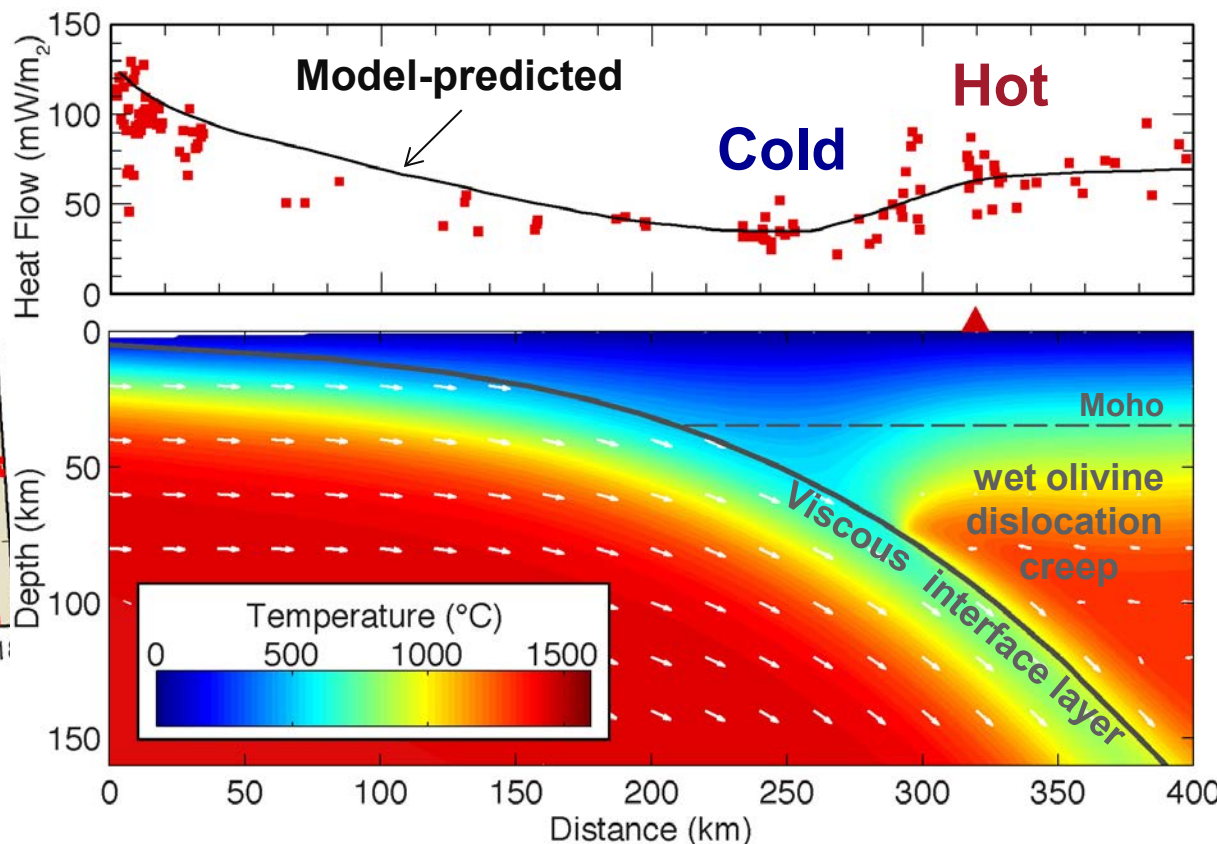


Slab age: 8Ma

Subduction rate: 43 mm/yr

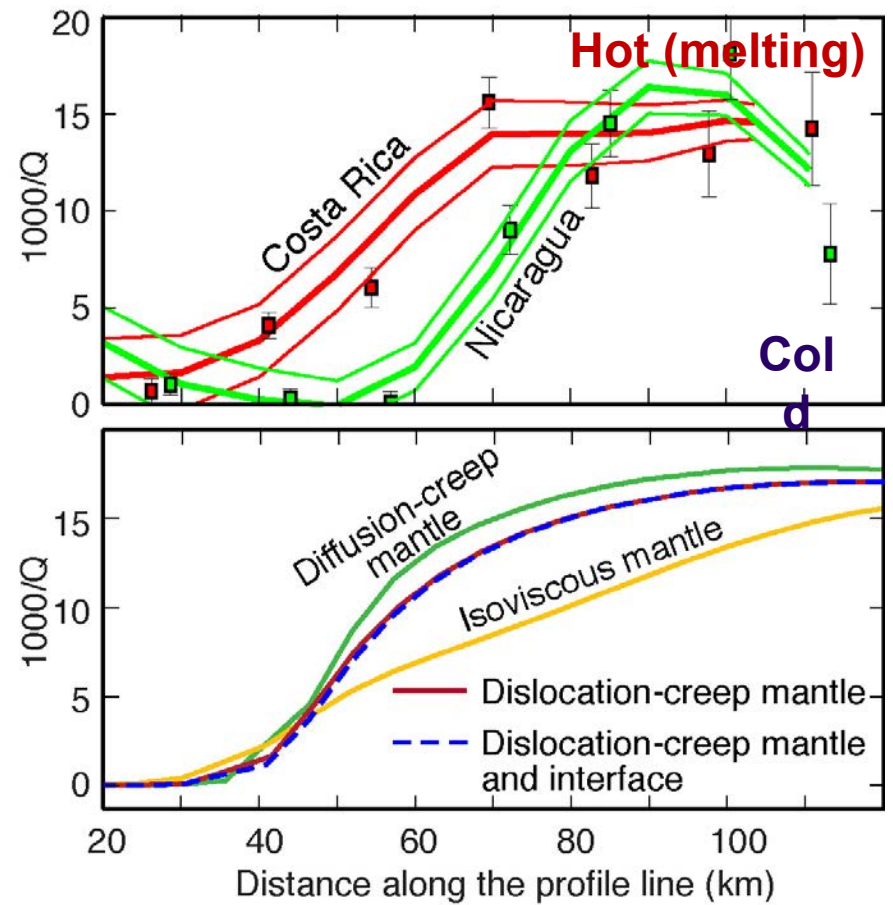
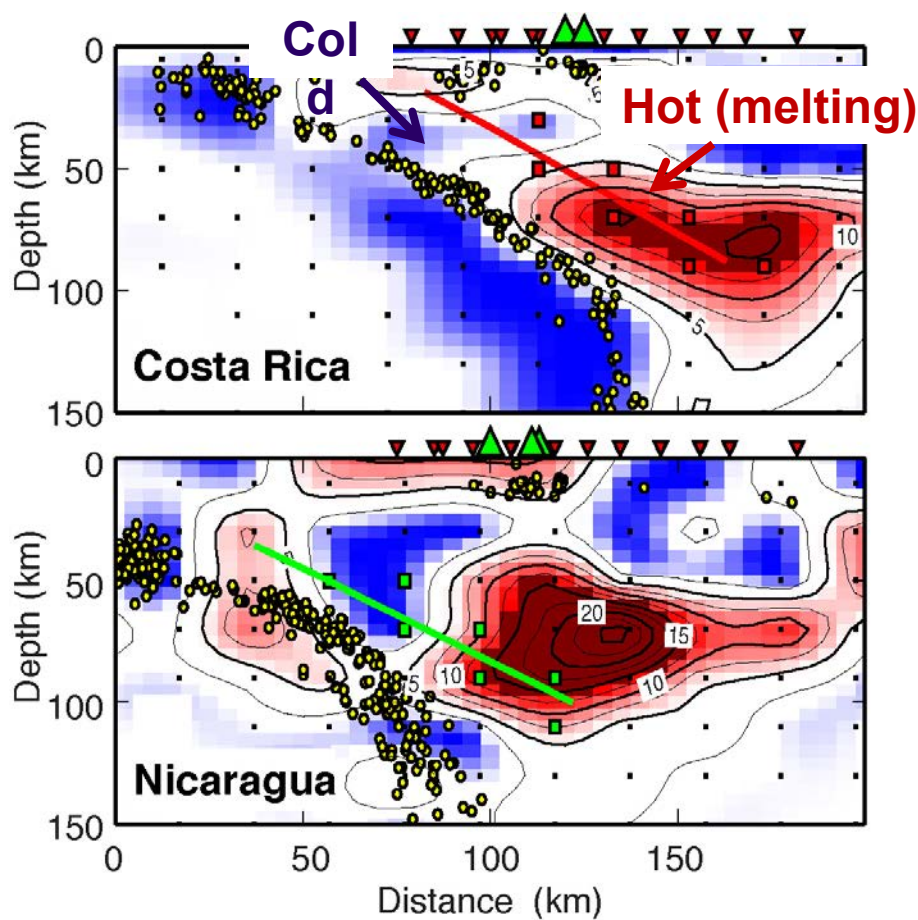
Frictional heating 0-15 km depths

Max. depth of slab-mantle decoupling: 75 km



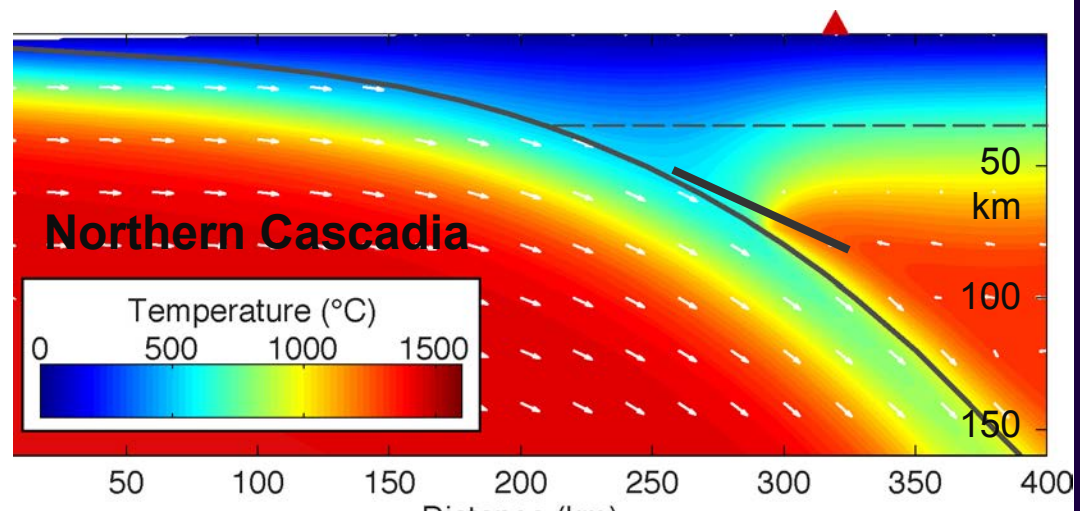
[Wada, Wang, He, & Hyndman, 2008]

- The decoupling-deepening transition is mainly due to a strong feedback between the lower temperature of the strength and viscous coupling, leading to a strong thermal contrast between the stagnant and flowing parts of the wedge.
- The MDD of 70-80 km satisfies low forearc surface heat flow and high mantle temperature (>1200 °C) in the sub-arc mantle.

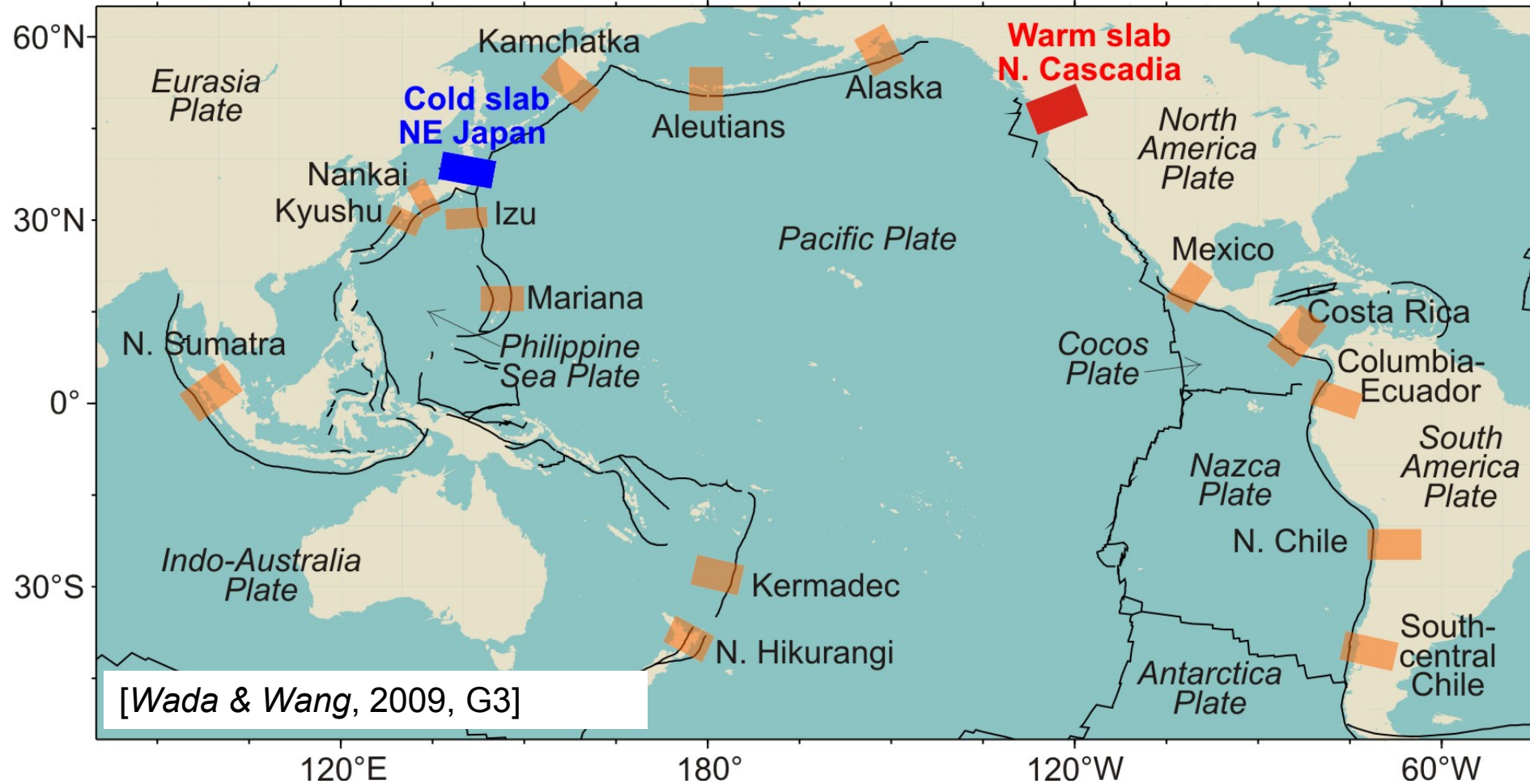


[Wada, Rychert, & Wang, 2011]

The sharp increase in the wedge temperature is consistent with the characteristic increase in seismic attenuation.

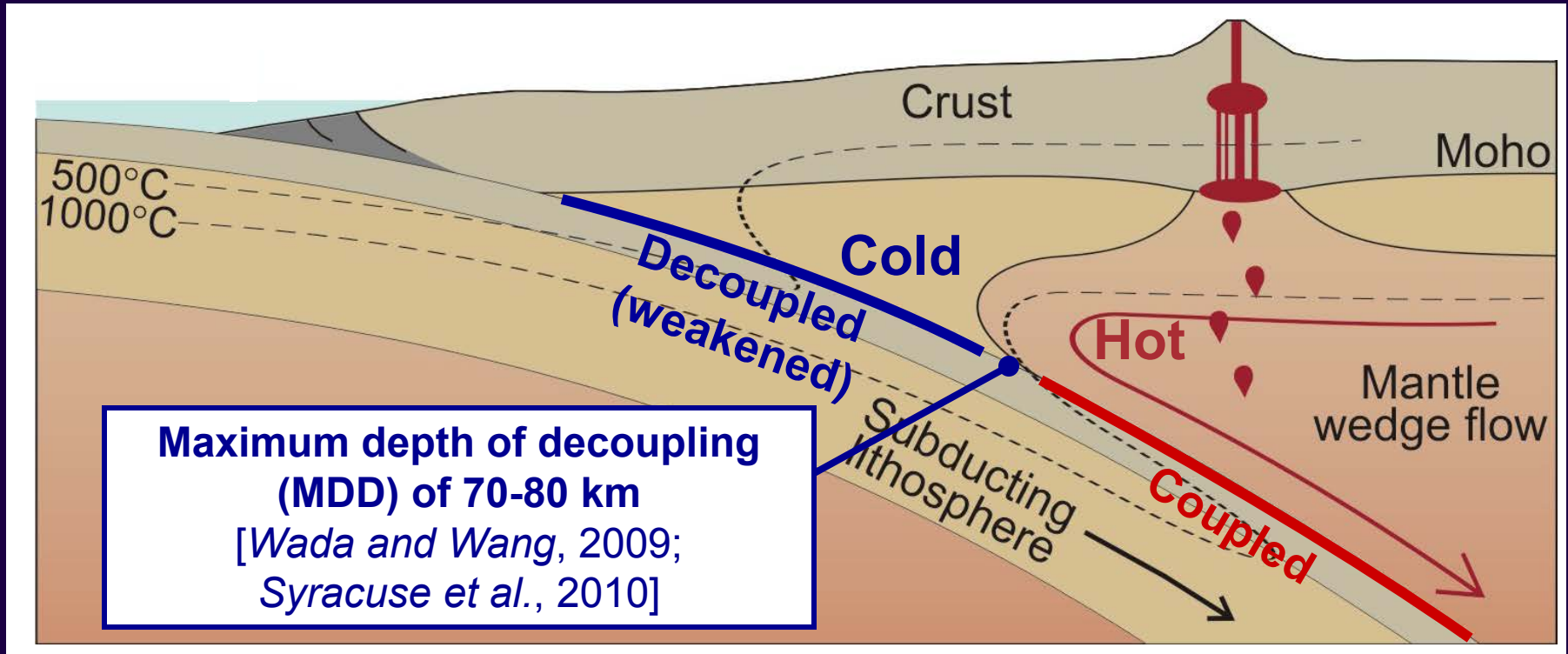


Common Maximum Depth of Decoupling



- The MDD is 70-80 km for most subduction zones [Wada & Wang, 2009; Syracuse et al., 2010]

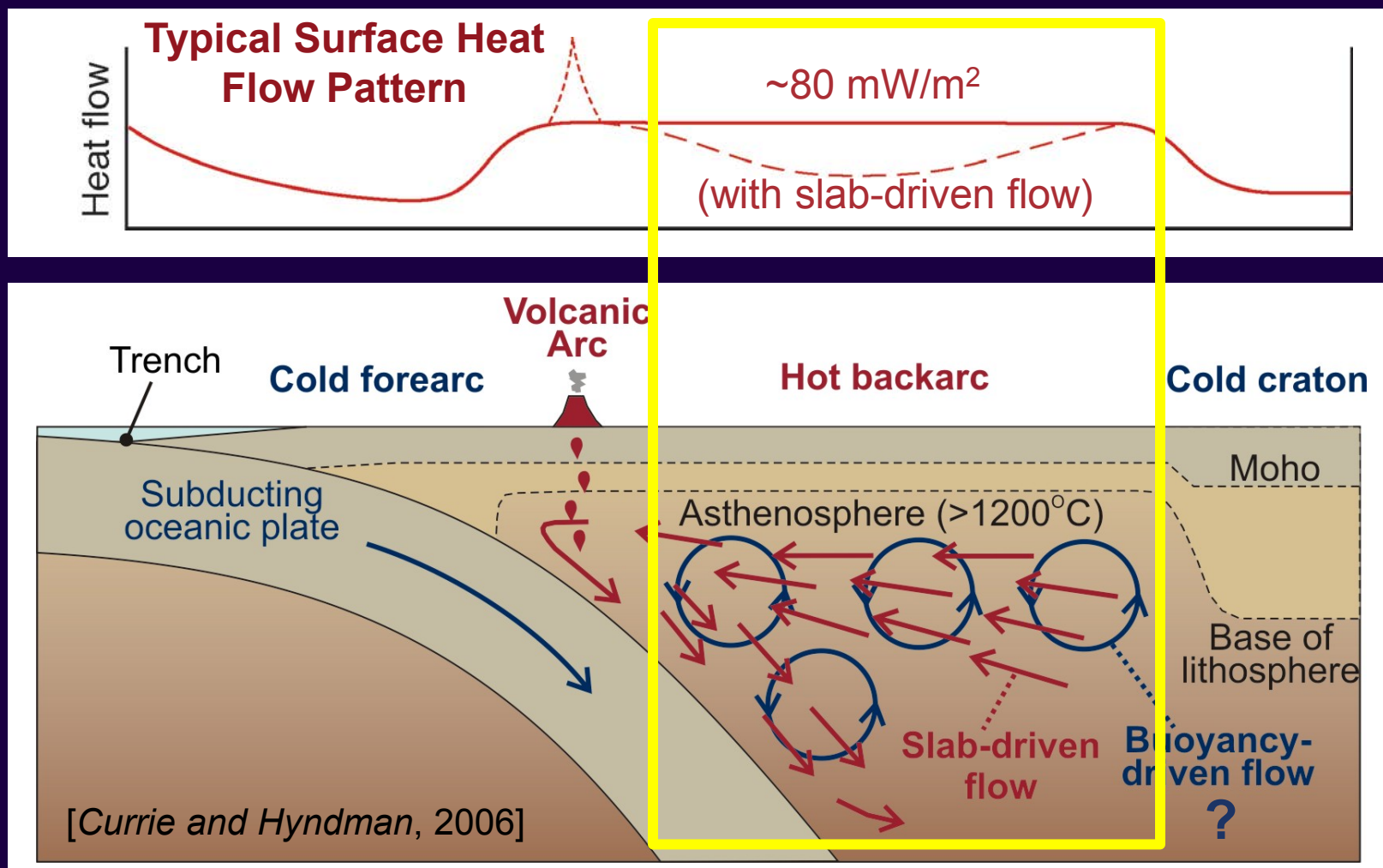
What controls the MDD?



Factors that affect the mantle-interface strength contrast

- T- dependence of the mantle and interface rheologies
- Metamorphic and dehydration/hydration reactions
- Fluid and melt contents, grain size, ...
- Mantle dynamics beneath the backarc
- ...

Mantle Flow beneath the Backarc

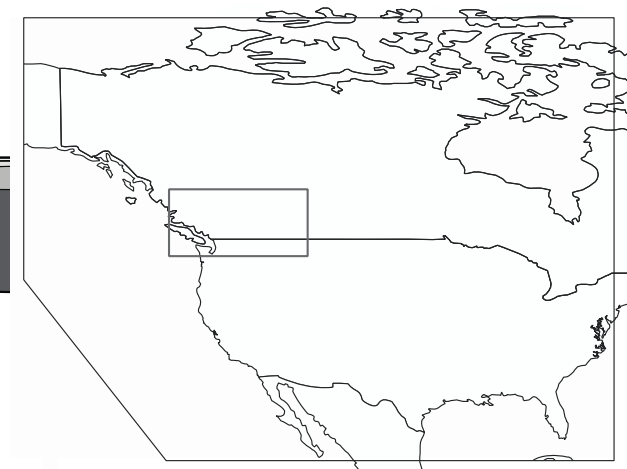
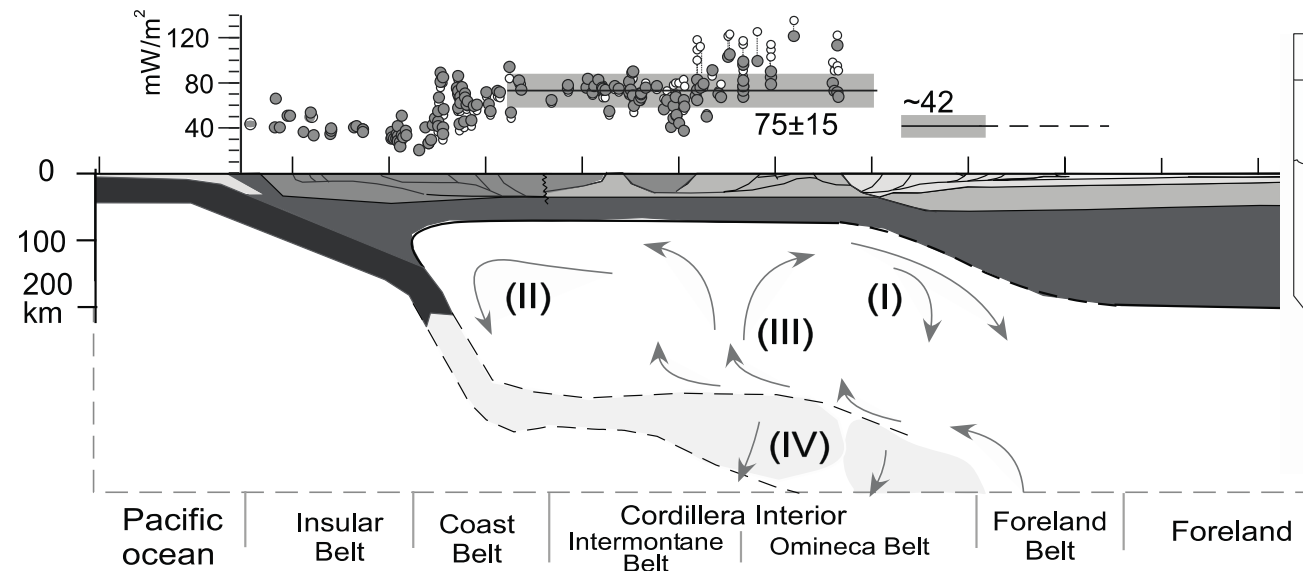
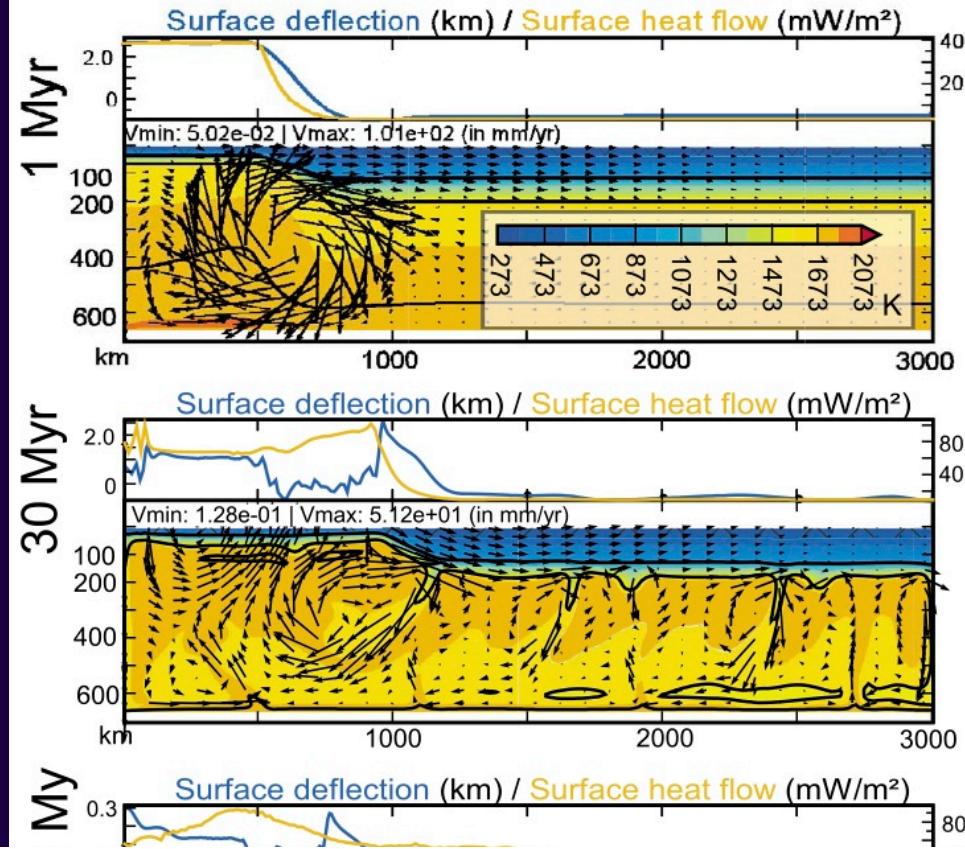


- Hot backarcs inferred from heat flow, seismic structure, and xenolith thermobarometry [Currie and Hyndman, 2006] cannot be maintained by corner flow.

Mantle Flow in the Backarc

Small-scale convection

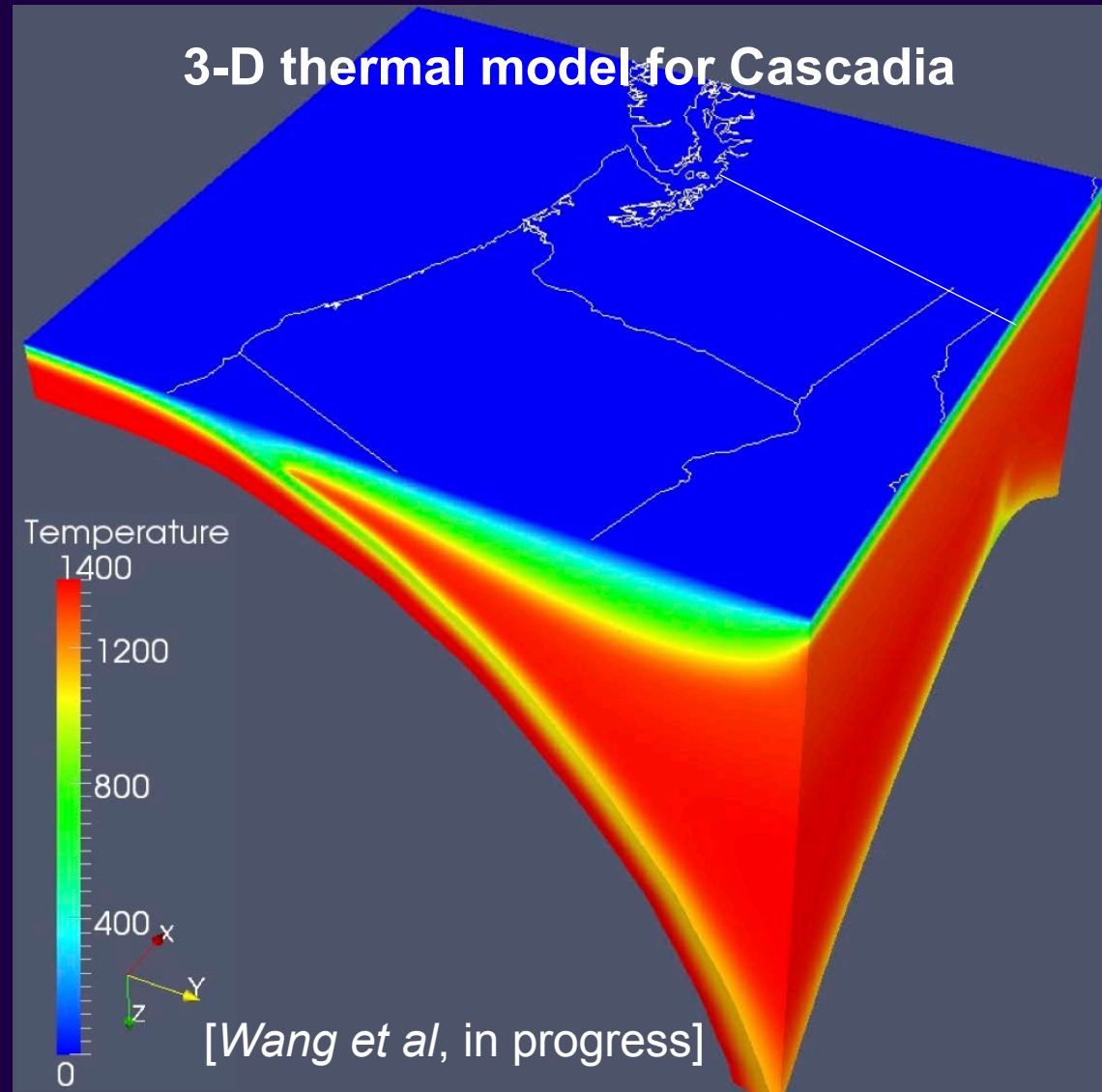
- Slab-driven flow and edge-driven flow [Hardebol et al., 2012]
- It affects the thermal state of the forearc and arc regions & geochemistry of arc magmas [e.g., Hall et al., 2012].



[Hardebol et al., 2012]

Competition between slab-driven flow and ...

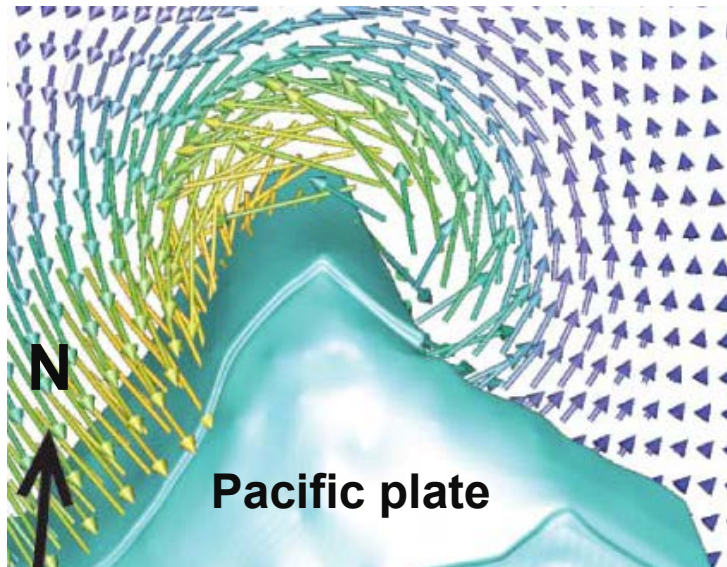
- Along-arc variations in slab geometry [e.g., *Kneller and van Keken, 2007*]



Competition between slab-driven flow and ...

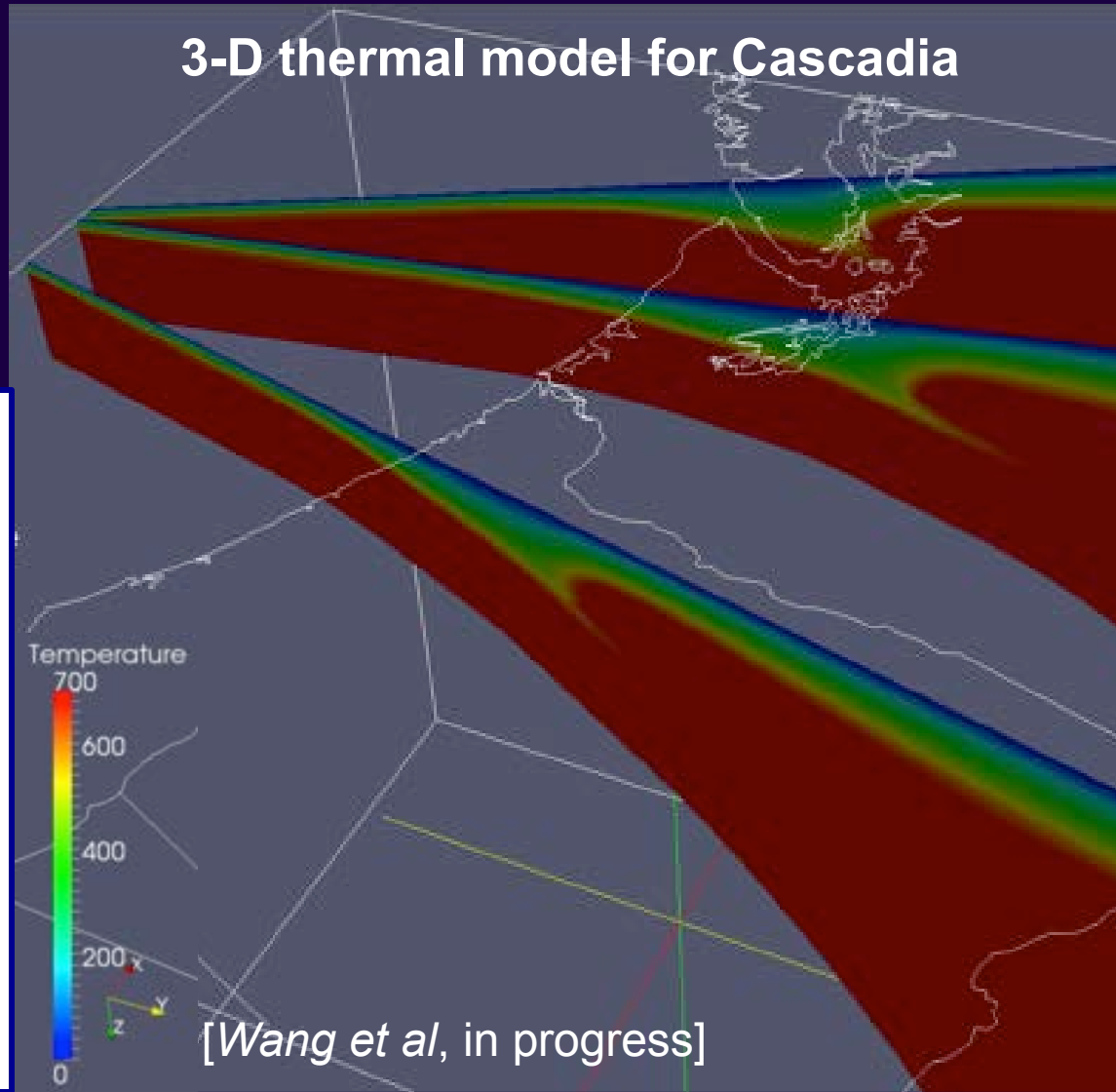
- Along-arc variations in slab geometry [e.g., *Kneller and van Keken, 2007*]
- Slab edge flow [*Jadamec and Billen, 2010*]
- Slab roll-back [*Long and Silver, 2008*]

Slab beneath central Alaska



[*Jadamec and Billen, 2010*]

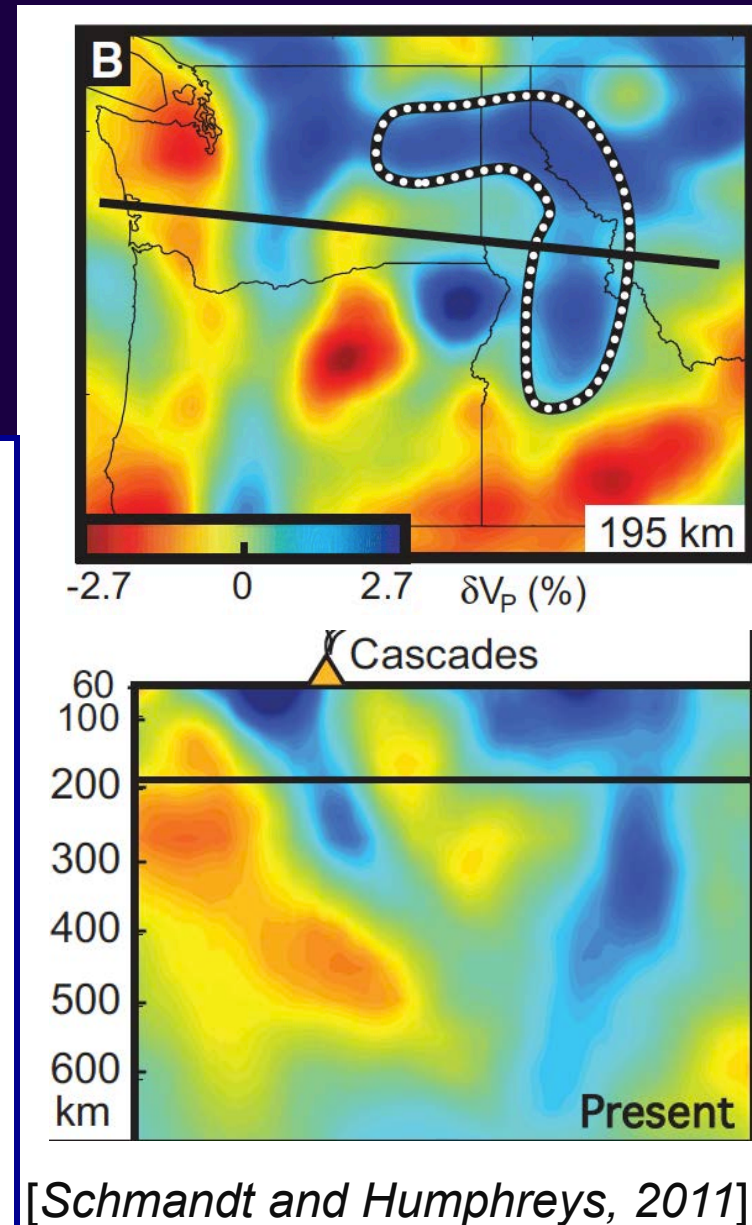
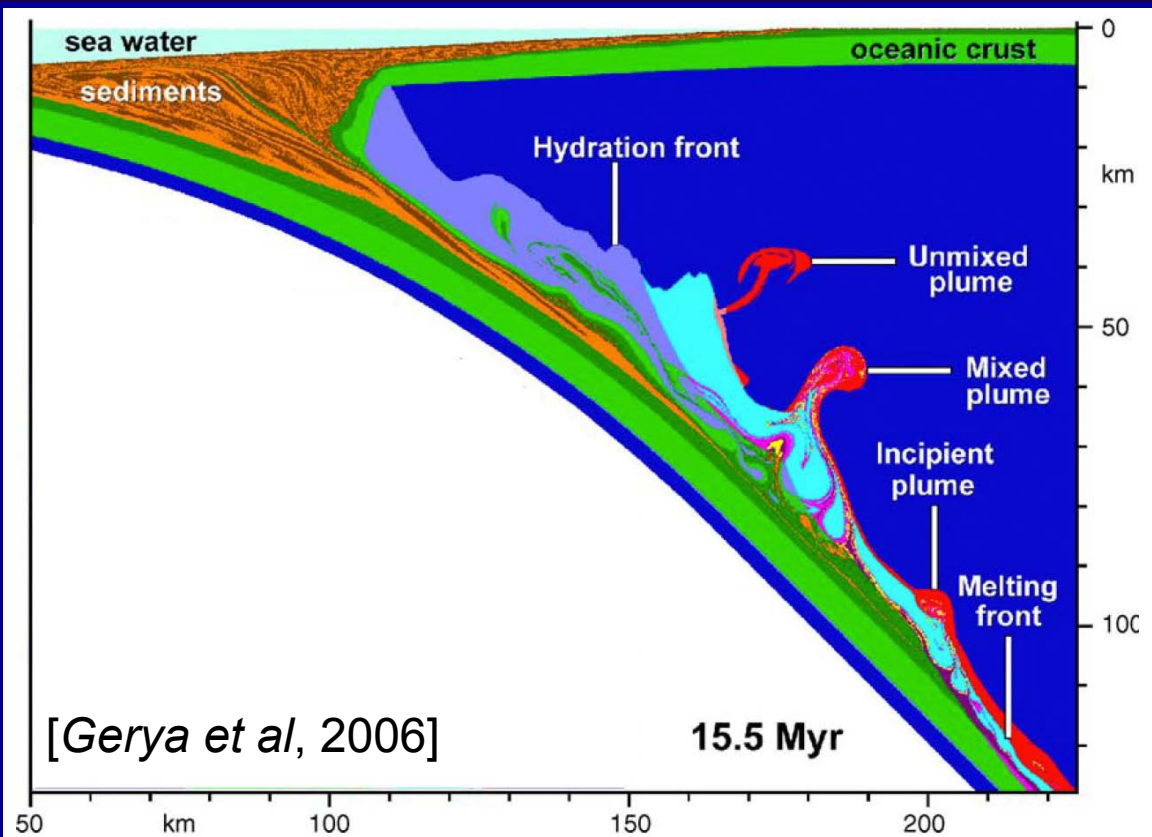
3-D thermal model for Cascadia



[*Wang et al, in progress*]

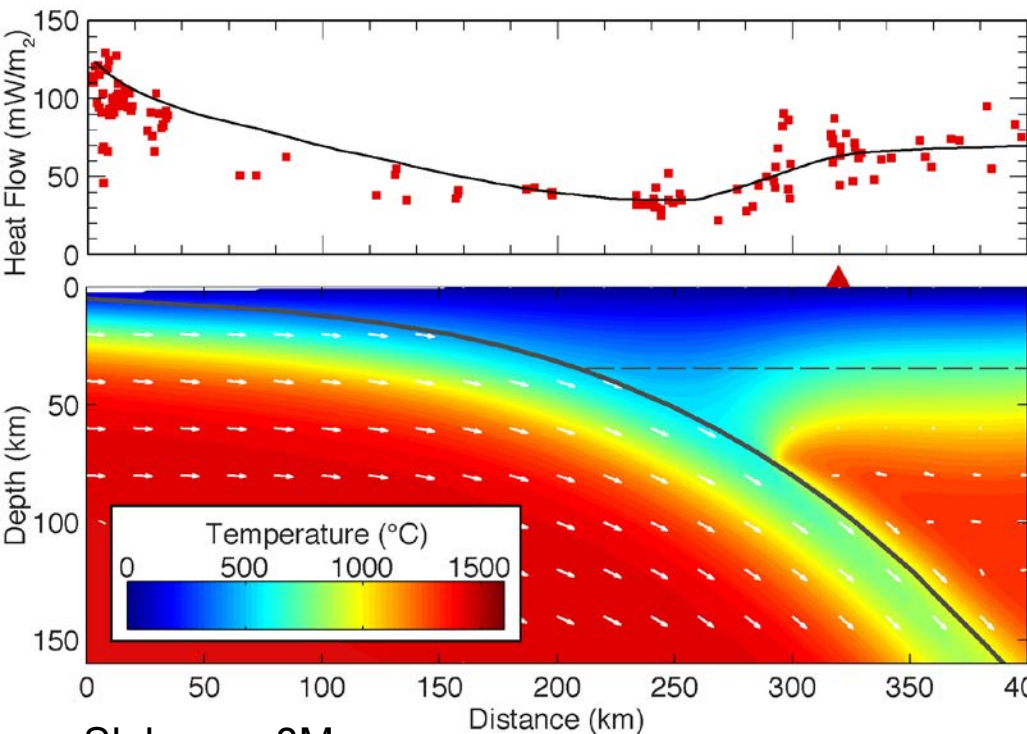
Competition between slab-driven flow and ...

- Structural obstacles
- “Cold plumes” [Gerya and Yuen, 2003, Gerya et al., 2006]
- Foundering of arc lower crust [Behn et al., 2007]...



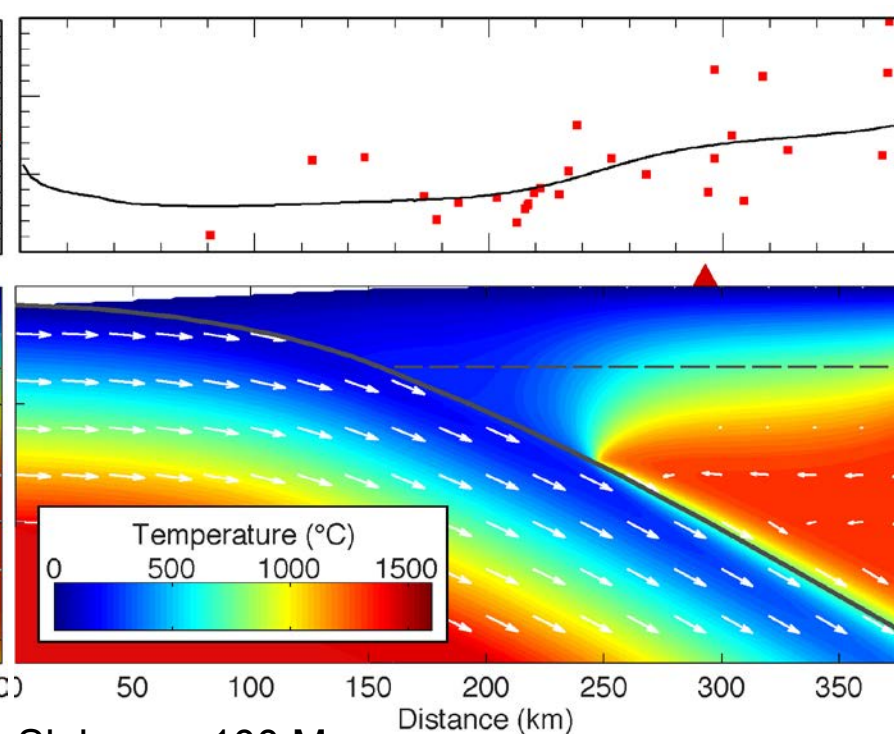
Thermal Structure

Northern Cascadia (Warm)



Slab age: 8Ma
Subduction rate: 43 mm/yr
Frictional heating 0-15 km depths
Max. depth of slab-mantle decoupling: 75 km

NE Japan (Cold)

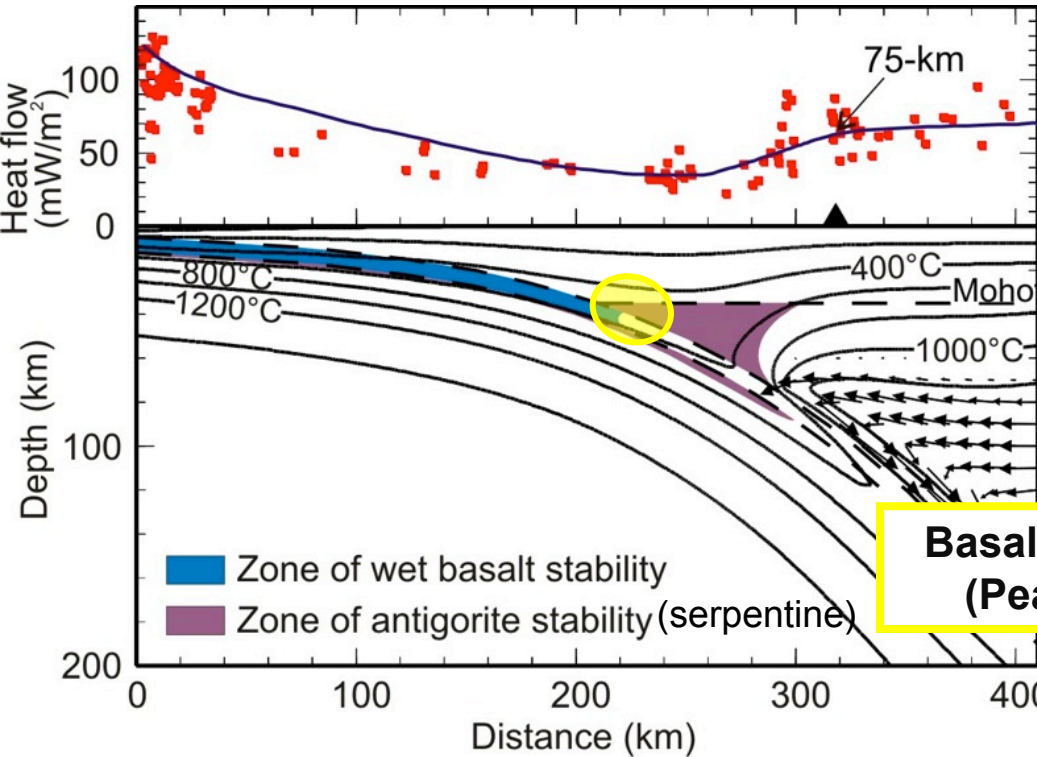


Slab age: 100 Ma
Subduction rate: 83 mm/yr
Frictional heating 0-40 km depths
Max. depth of slab-mantle decoupling: 75 km

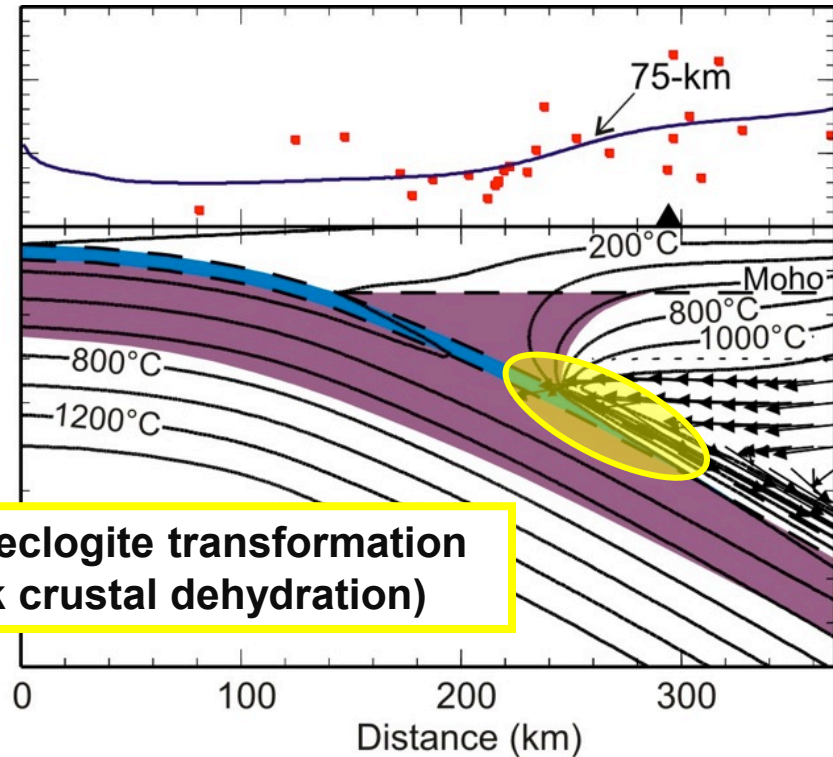
[Modeling results from *Wada and Wang, 2009, G3*]

Petrologic Structures

Cascadia (warm 8-Ma slab)



NE Japan (cold 100-Ma slab)



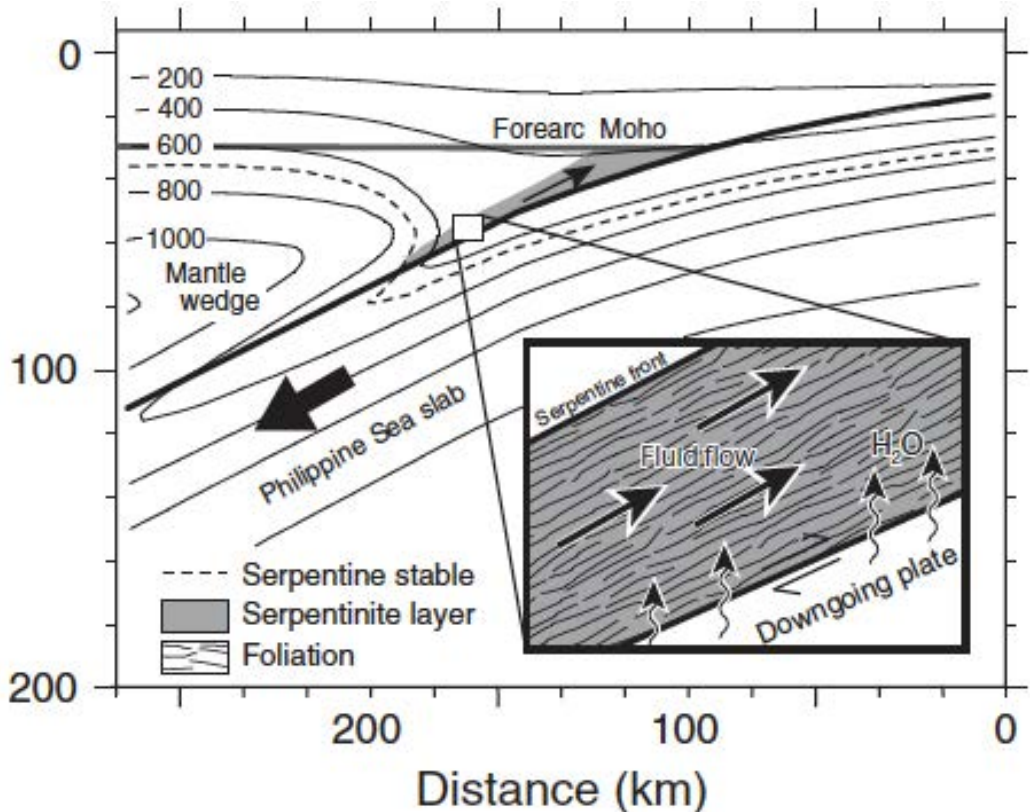
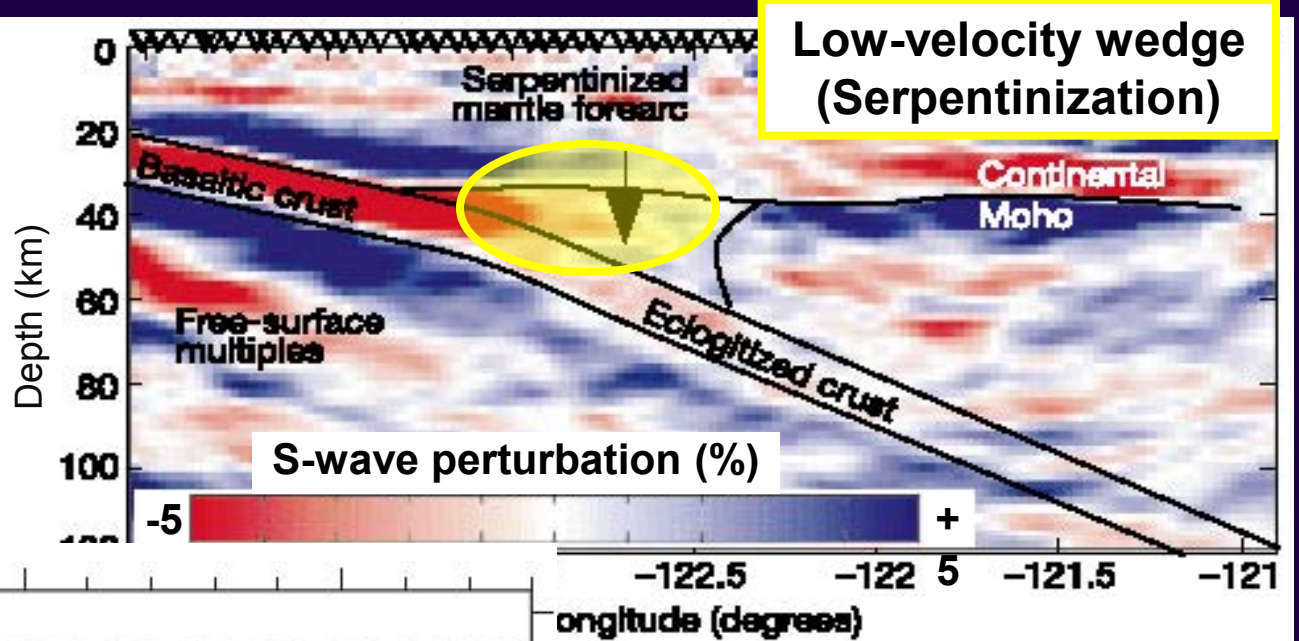
**Basalt-eclogite transformation
(Peak crustal dehydration)**

[Wada and Wang, 2009, G3]

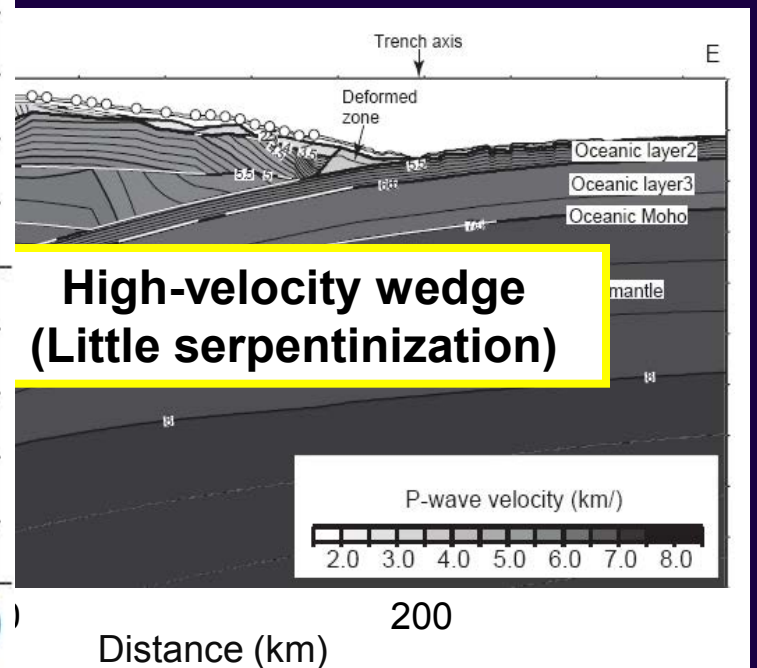
- Shallower peak crustal dehydration in Cascadia
- Thinner zone of serpentine stability in the Juan de Fuca slab
- Zone of serpentine stability in the stagnant wedge in both

Cascadia (warm slab)

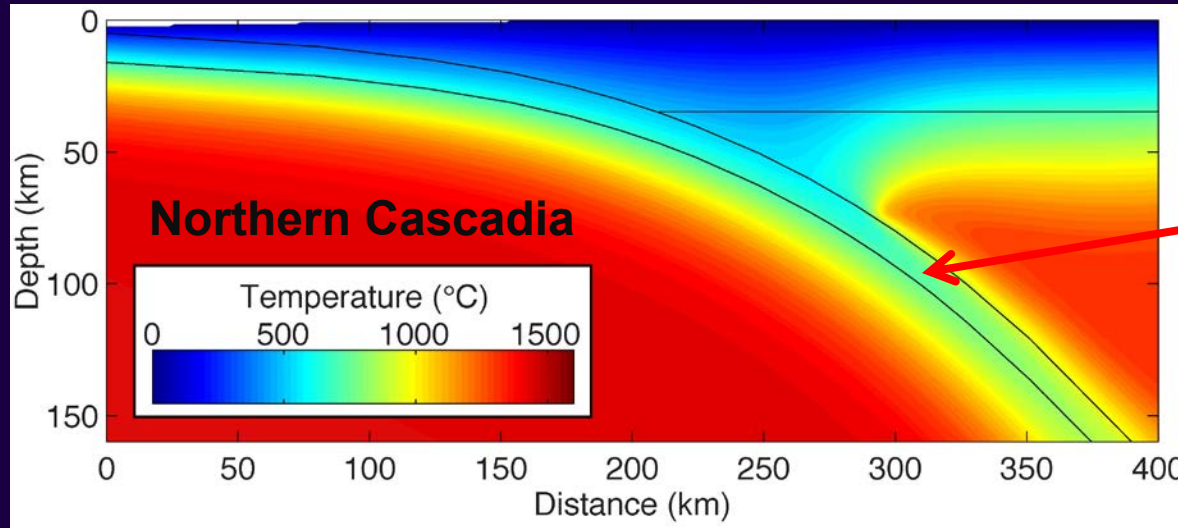
[Bostock et al., 2002]



[Kawano et al., 20011]



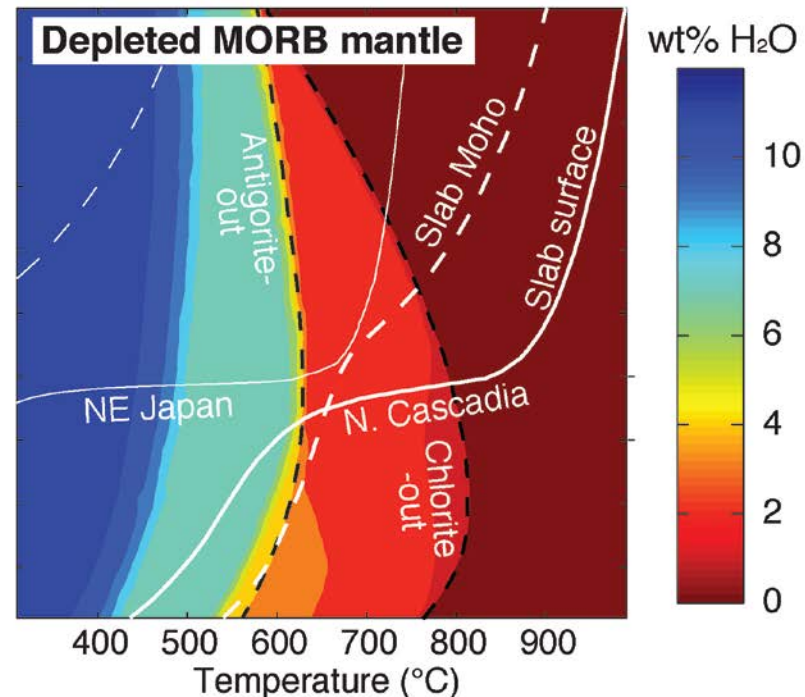
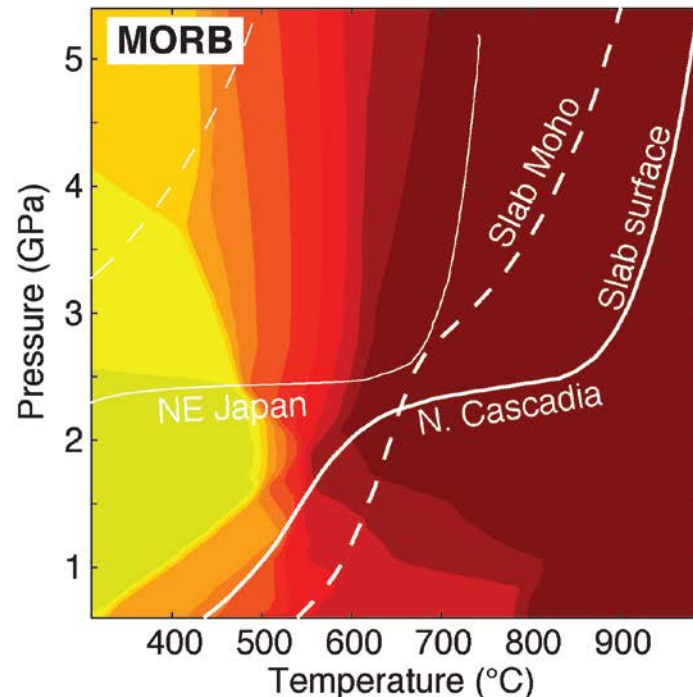
Pattern of H₂O Release from the Slab



Lithologies & H₂O contents in the top 11 km of the slab:

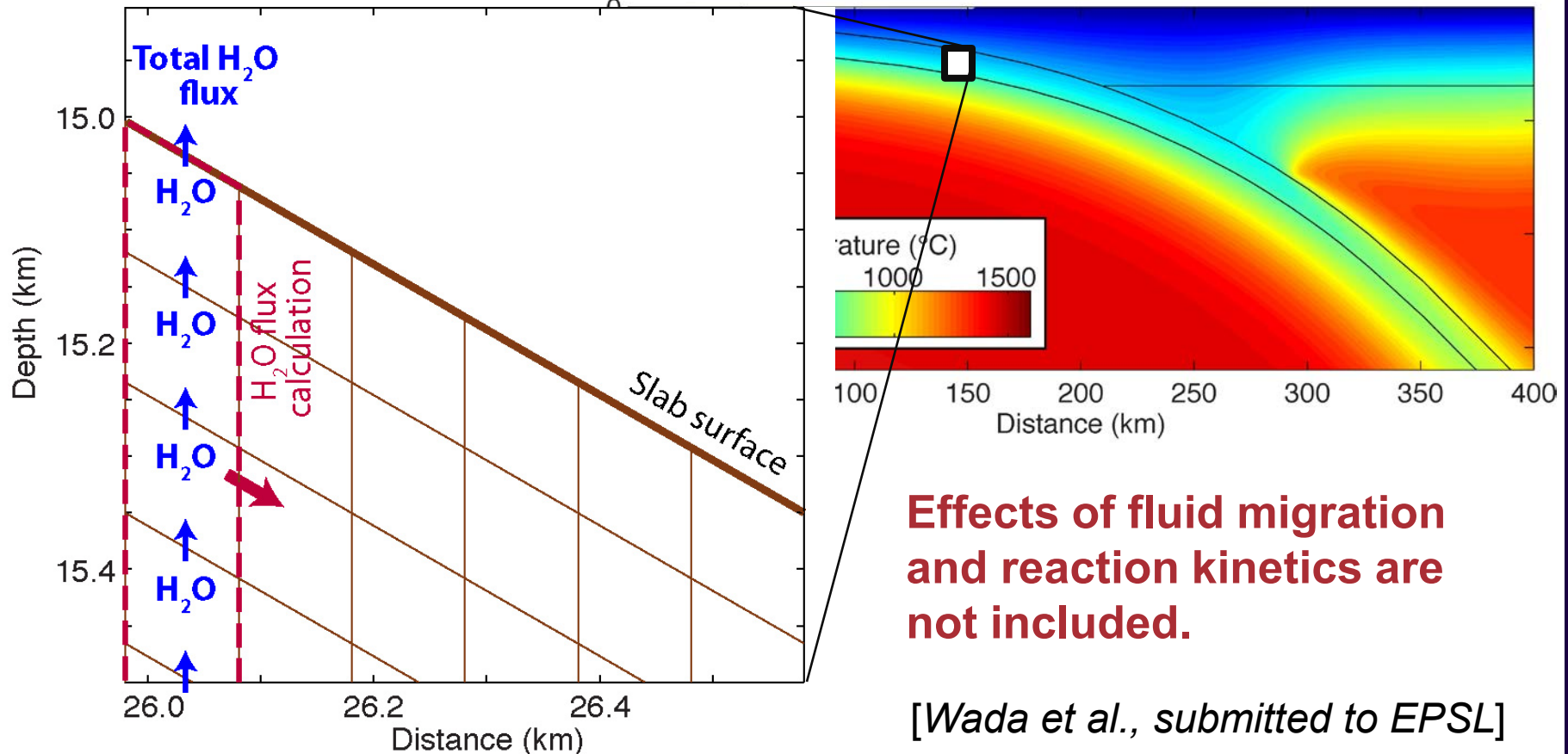
0.6 km volcanics	2.1 wt%
1.4 km dykes	1.8 wt%
5 km gabbros	0.8 wt%
4 km peridotite	2.0 wt%

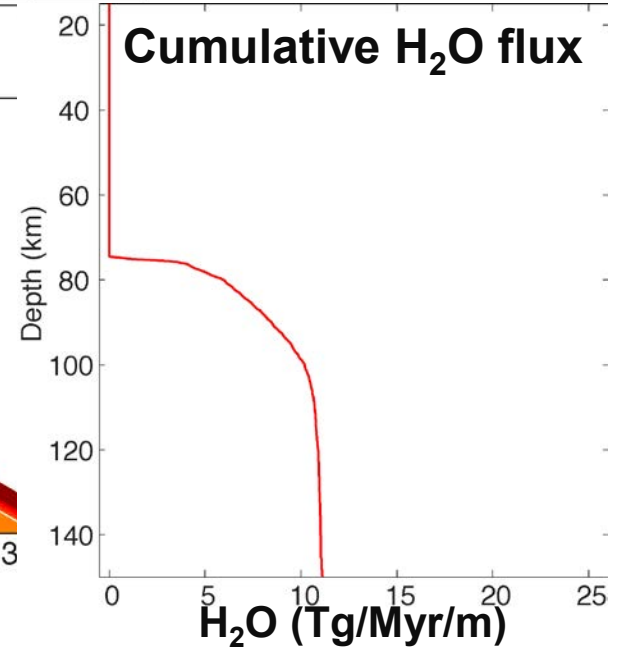
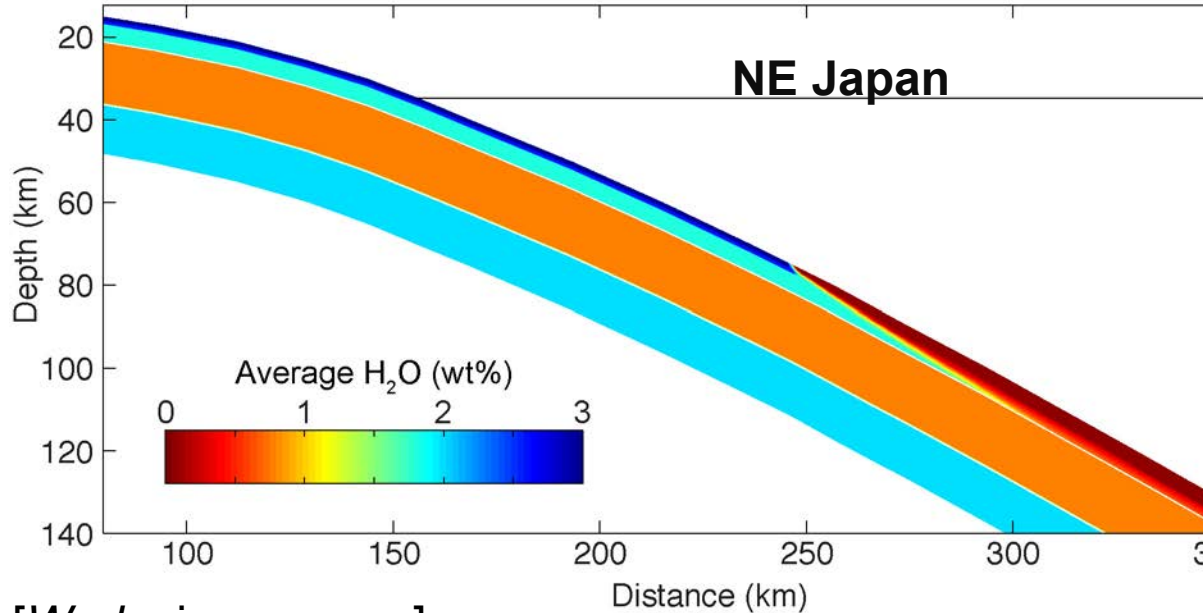
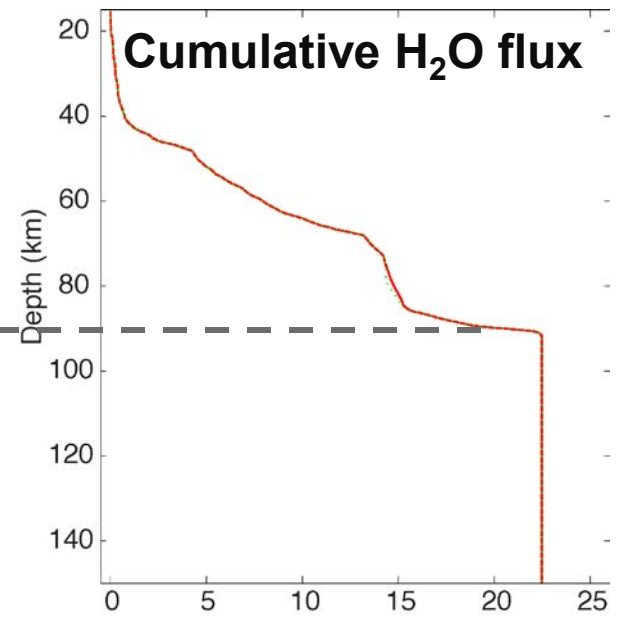
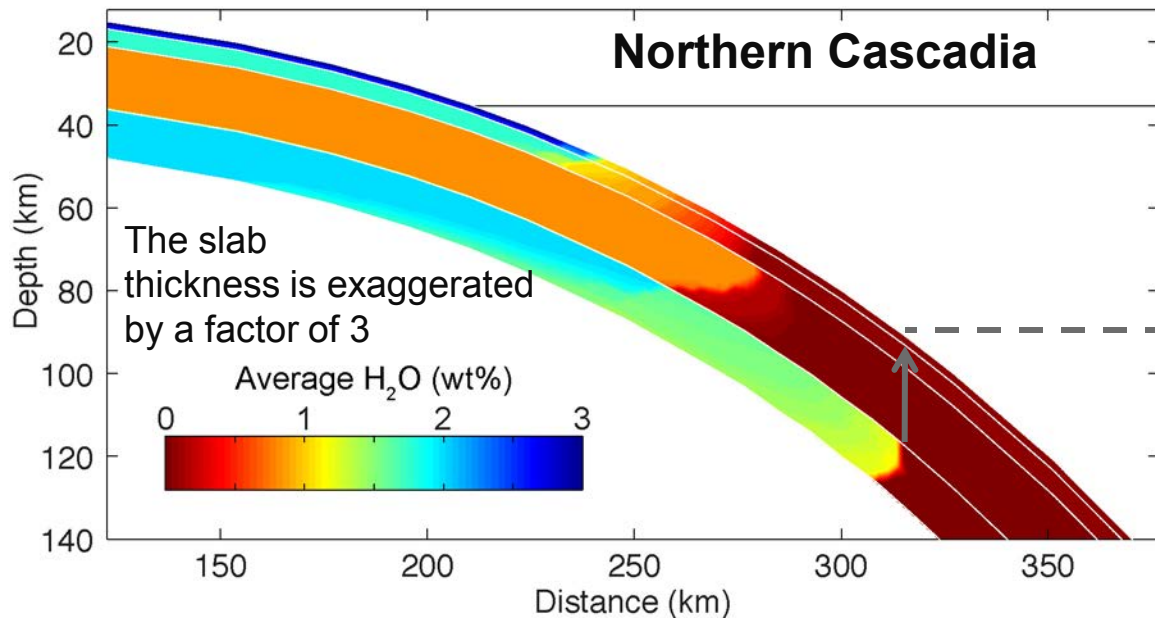
Thermodynamic Calculations by using Perple_X [Connolly, 2009]



Fluid Flux Calculations

- 11-km-thick section of the slab is divided into 100-m-wide vertical columns, each consisting of 100-m-thick elements.
- H_2O release is calculated in the shallowest column, and the updated H_2O contents of the column is passed down-dip.

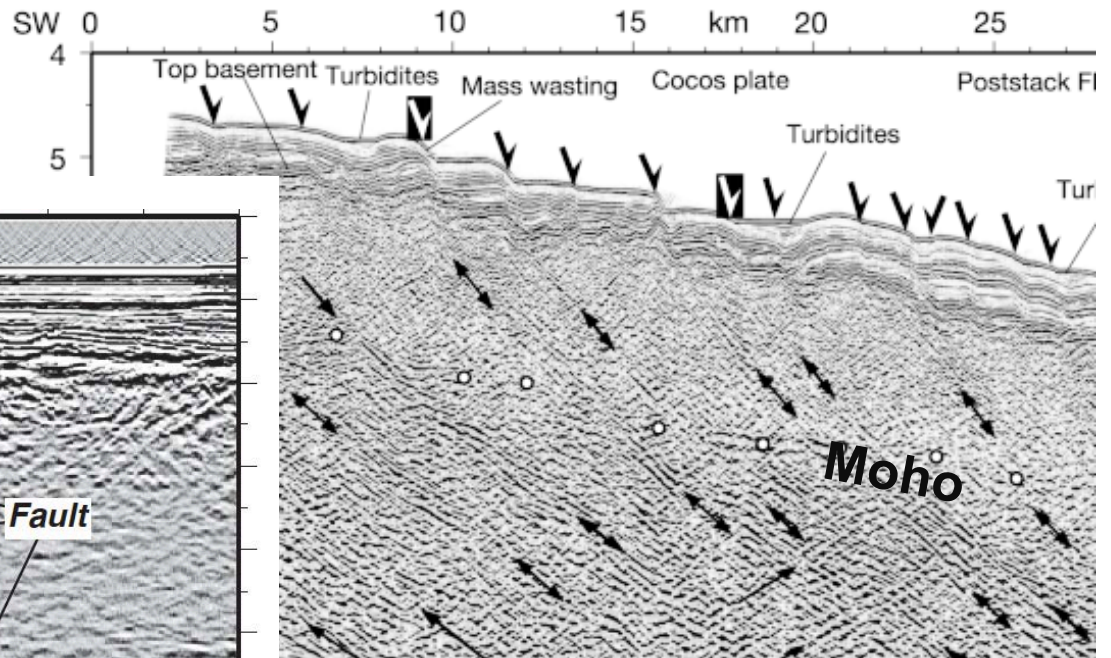




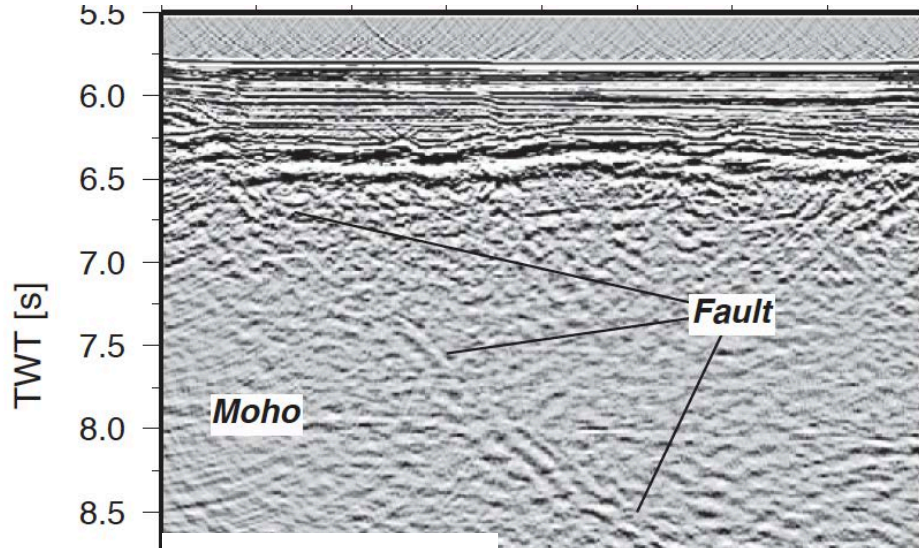
[Wada, in progress]

See *Hacker* [2008] and *van Keken et al.* [2011] on Global H₂O flux

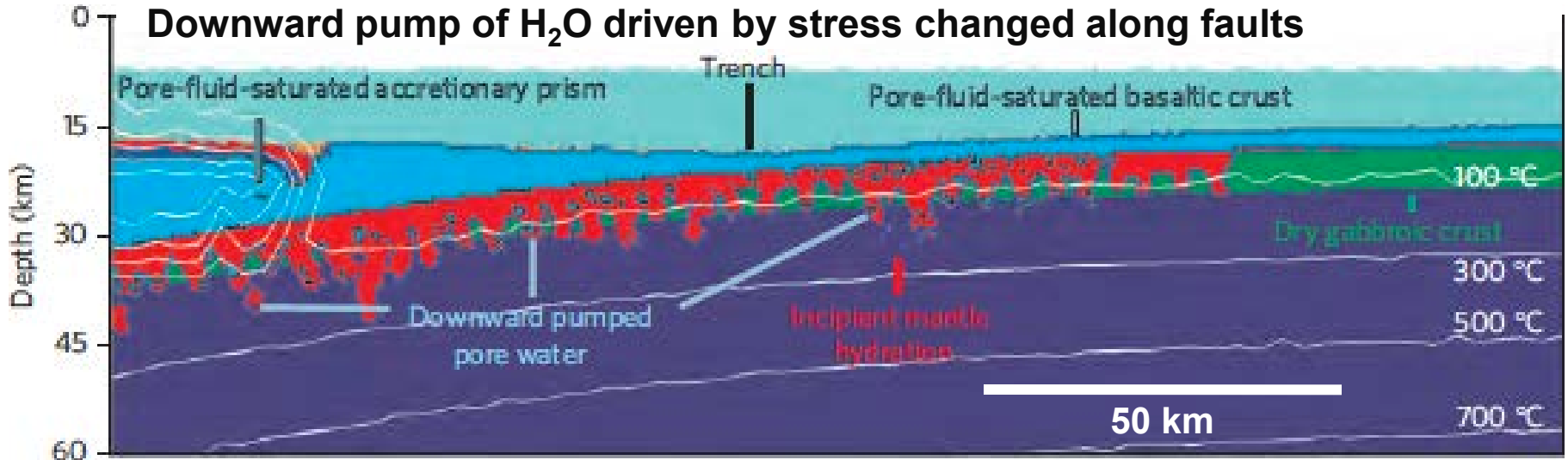
Localized hydration in the Incoming Plate



[Ranero et al, 2003]

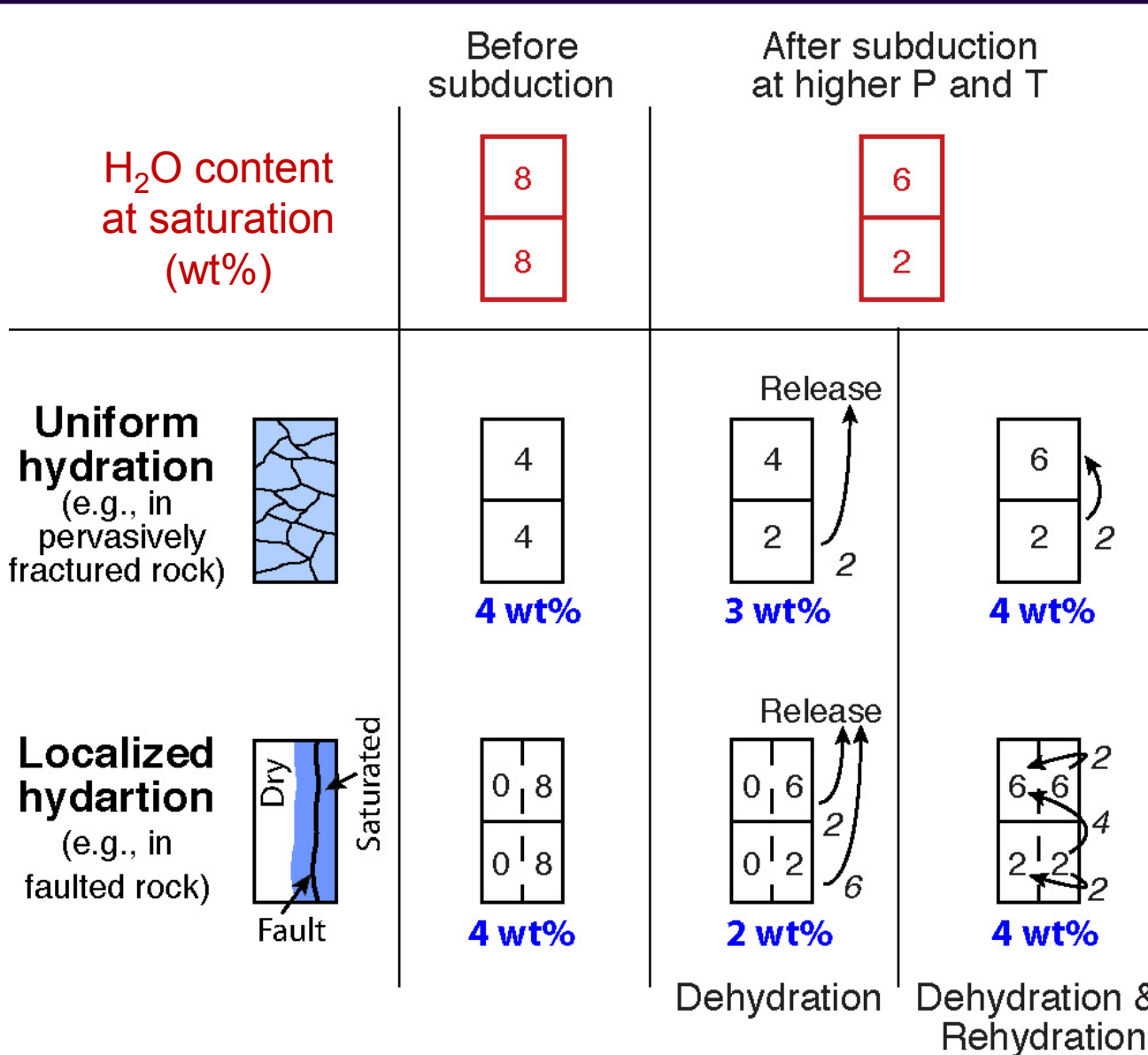


Downward pump of H₂O driven by stress changed along faults



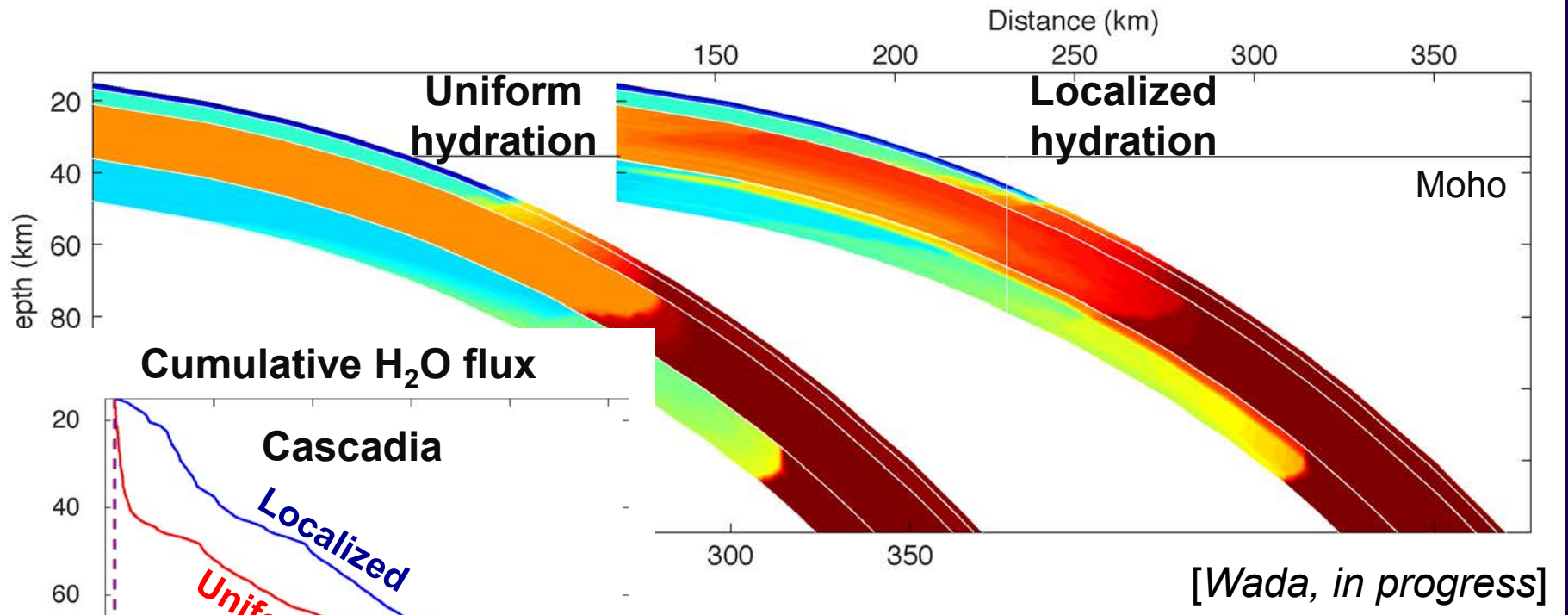
[Faccenda et al, 2009]

Localized Hydration and Rehydration



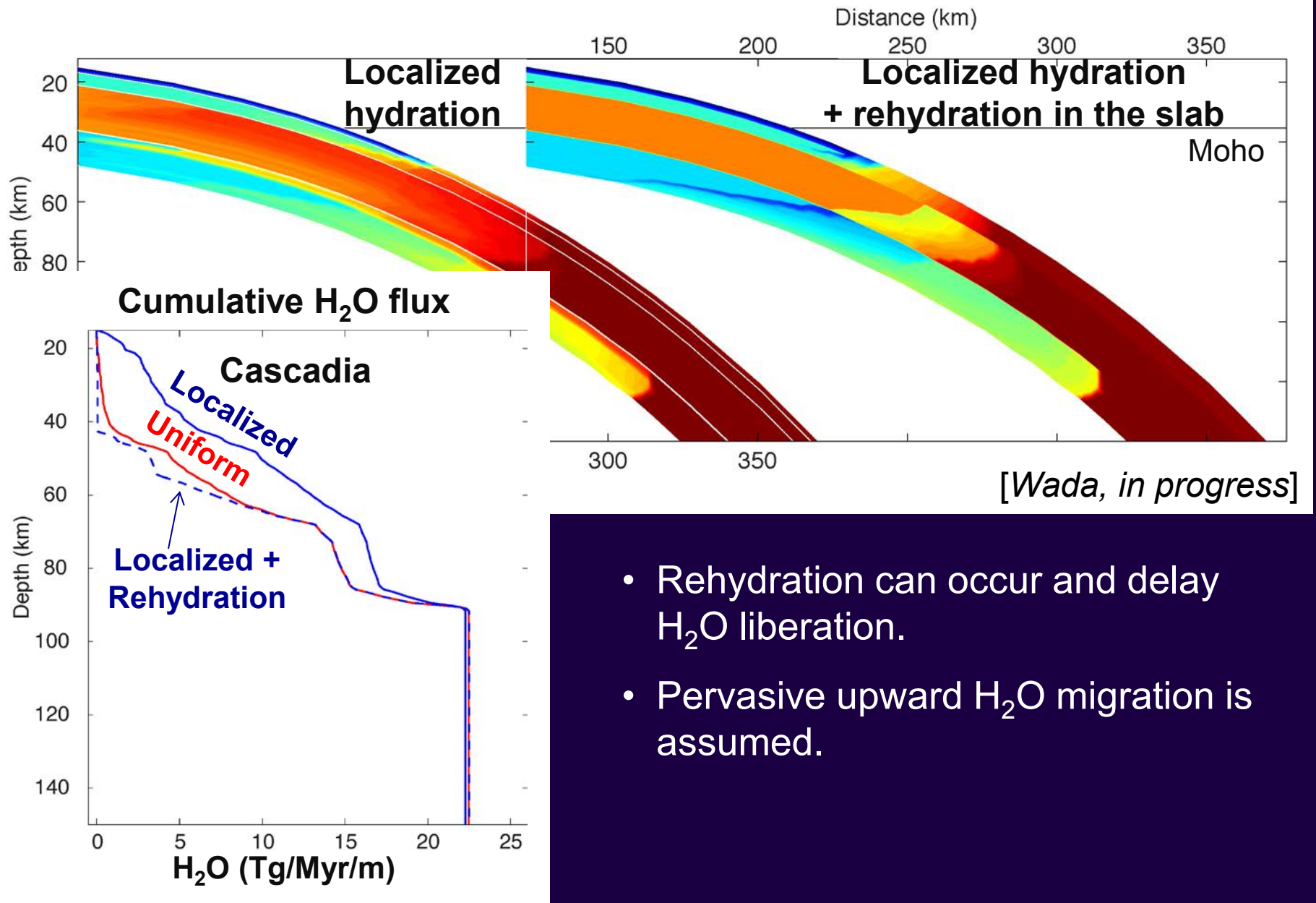
[Wada et al., submitted to EPSL]

Effects of Localized Hydration in the Incoming Plate



- Shallower H₂O release from lower crust and upper mantle in the locally hydrated slab.
- The degree of hydration affects the H₂O budget in the forearc and arc.

Effects of Rehydration in the Slab



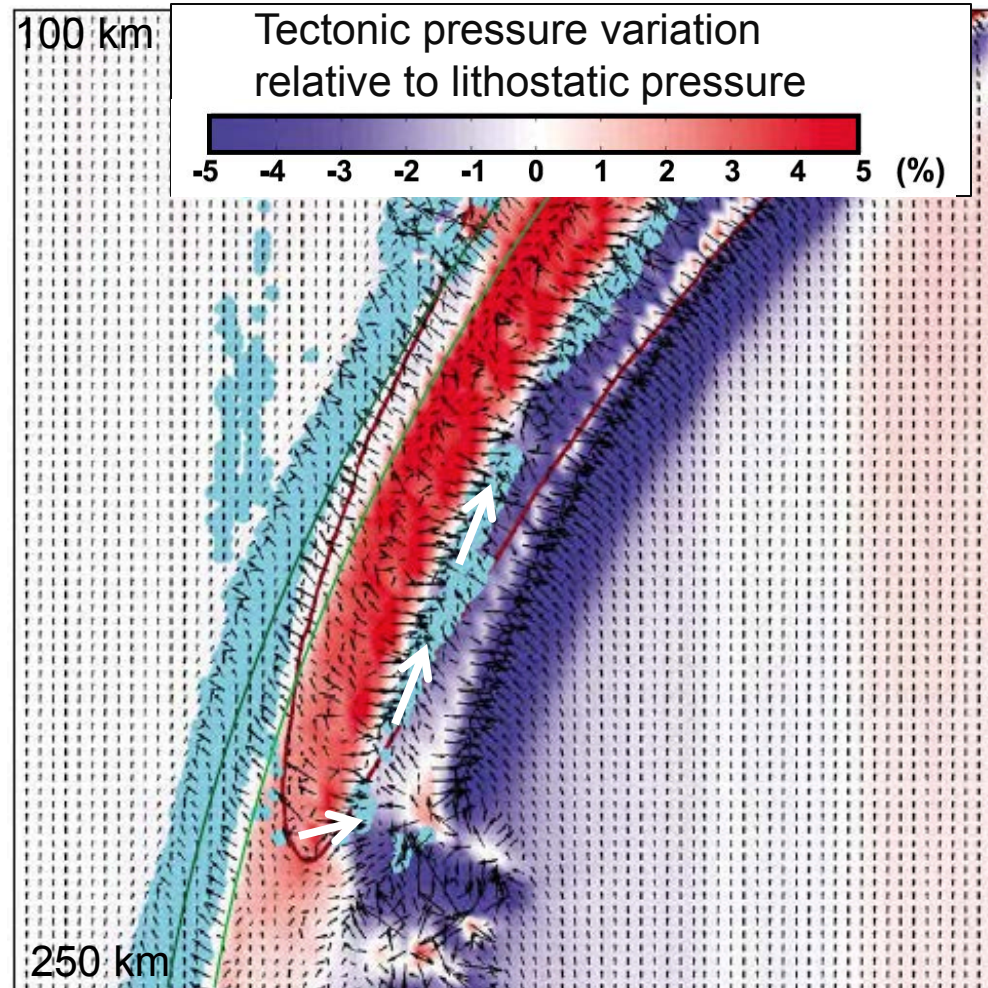
- Rehydration can occur and delay H₂O liberation.
- Pervasive upward H₂O migration is assumed.

Fluid Migration Path in the Slab



[Zack and John, 2007]

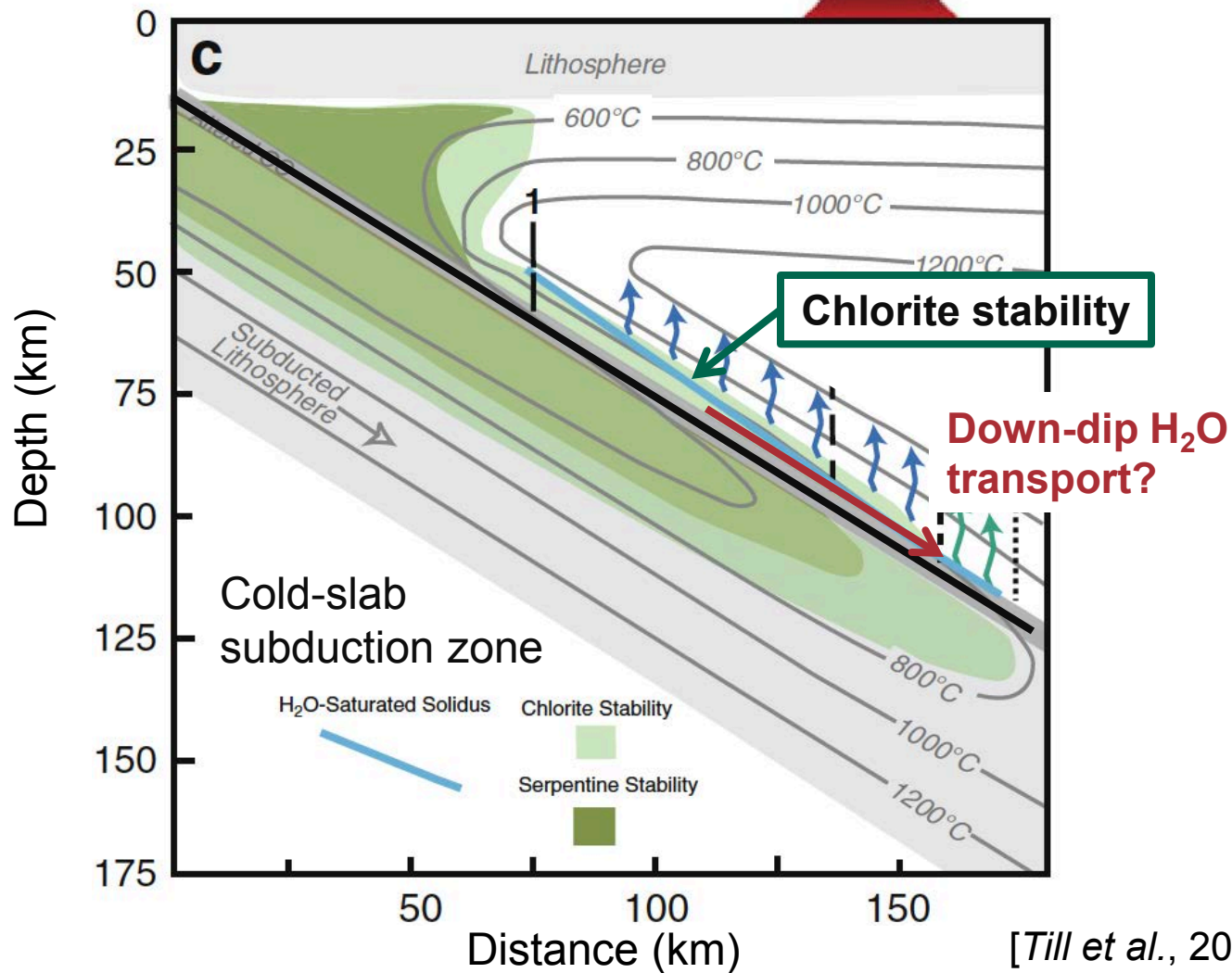
- The degree of rehydration depends on fluid migration path, which is influenced by factors such as vein/fracture network, tectonic pressure.



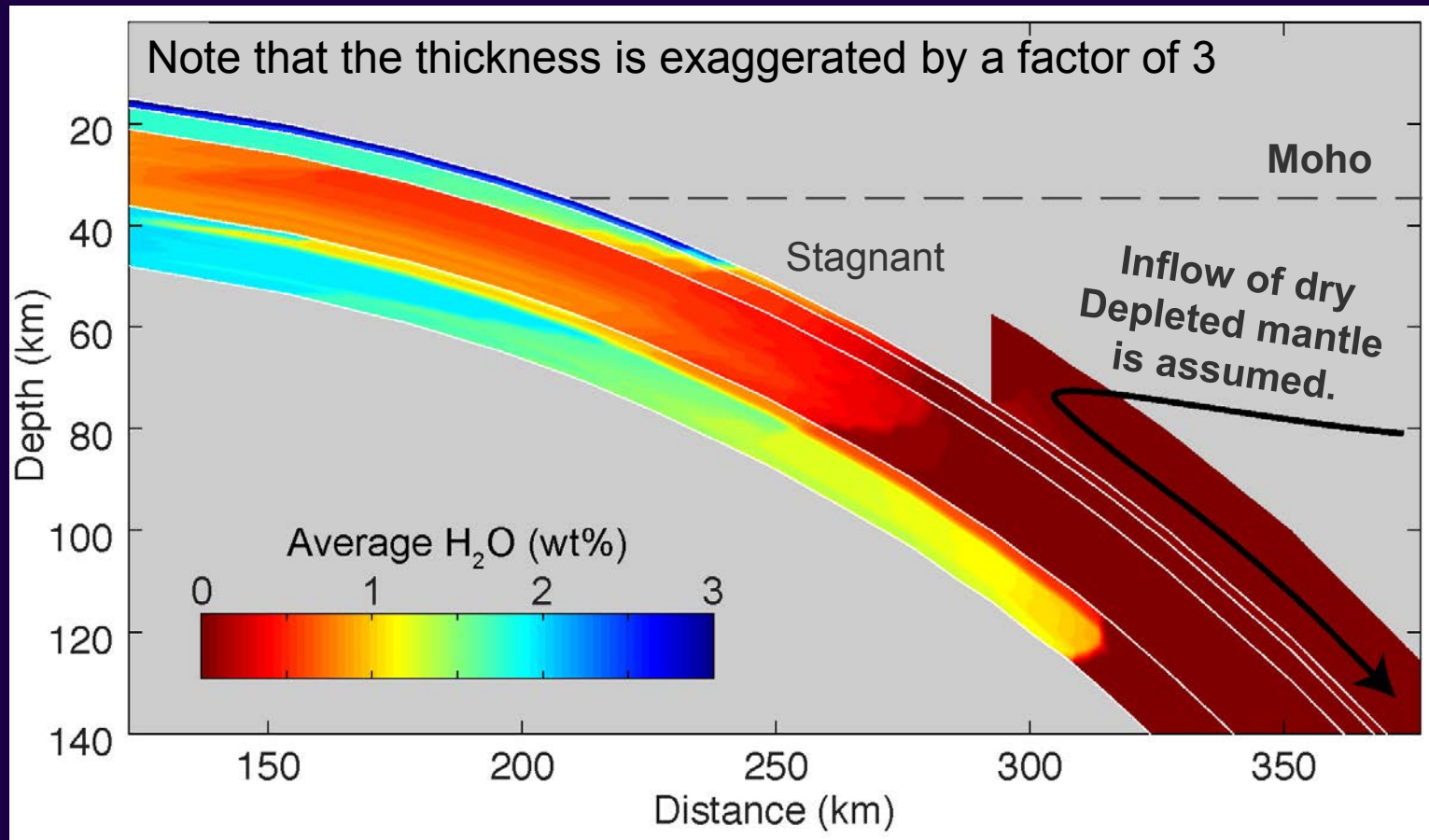
Faccenda et al., 2012

Hydration in the Overlying Mantle Wedge

Chlorite Stability in the Mantle Wedge



Effects of Hydration in the Overlying Flowing Mantle

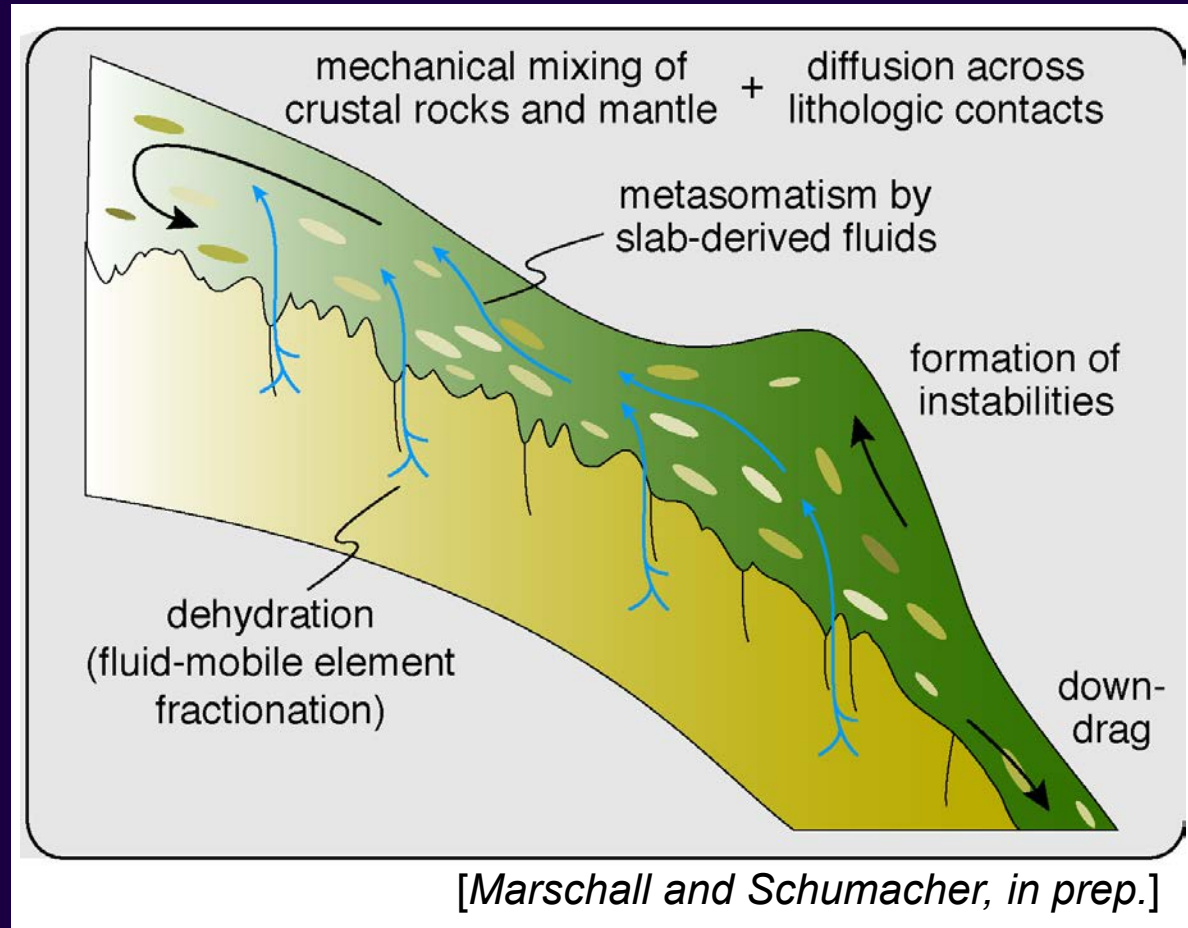


- The overlying mantle is too hot for a significant degree of hydration to occur.

Subduction Channel Mélange

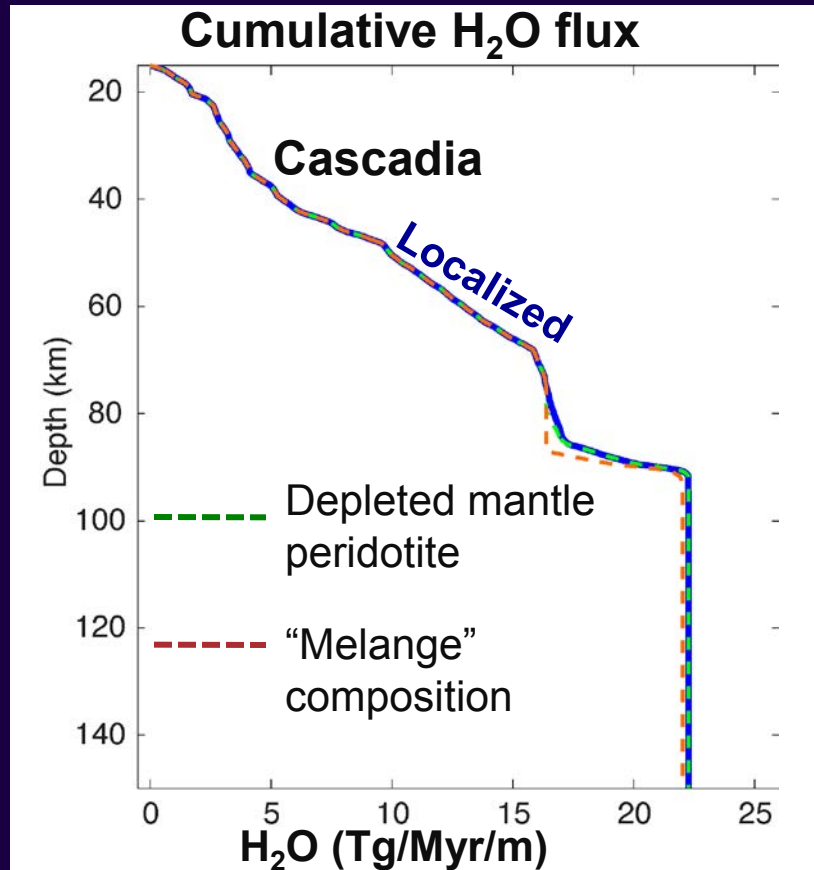
Compositional variations of the subduction interface material due to...

- Mechanical mixing with the subducted sediments and crust
- Addition of slab-derived Si- and Al-rich fluids



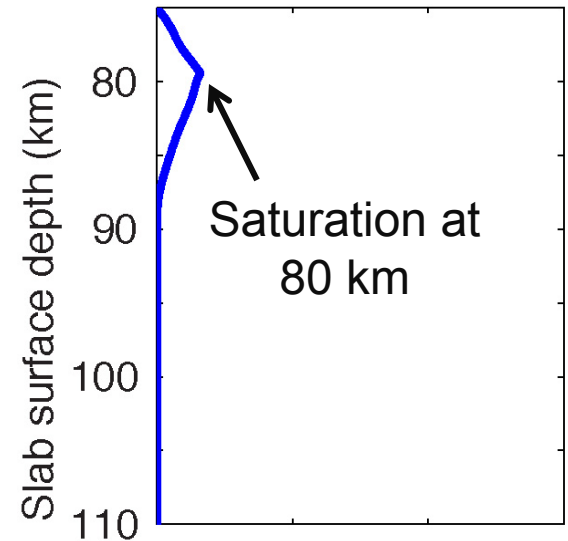
Subduction Channel Mélange

- The mélange composition can take up more H₂O and delays H₂O liberation further down-dip.
- H₂O uptake occurs over a narrow depth range.

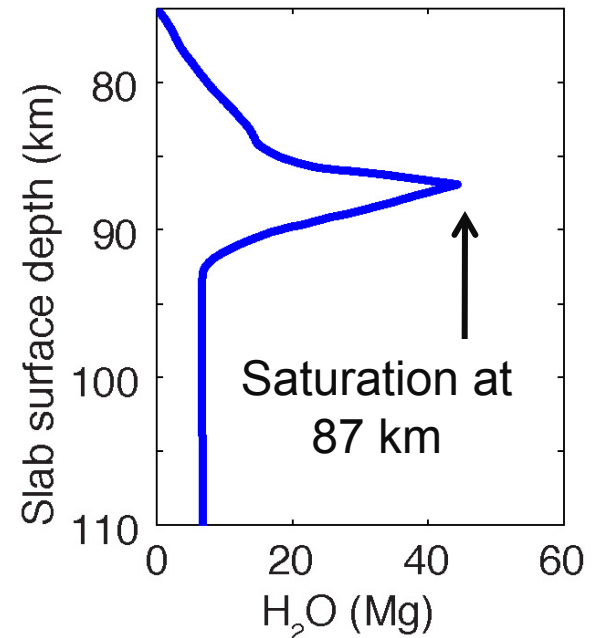


H₂O in the overlying mantle

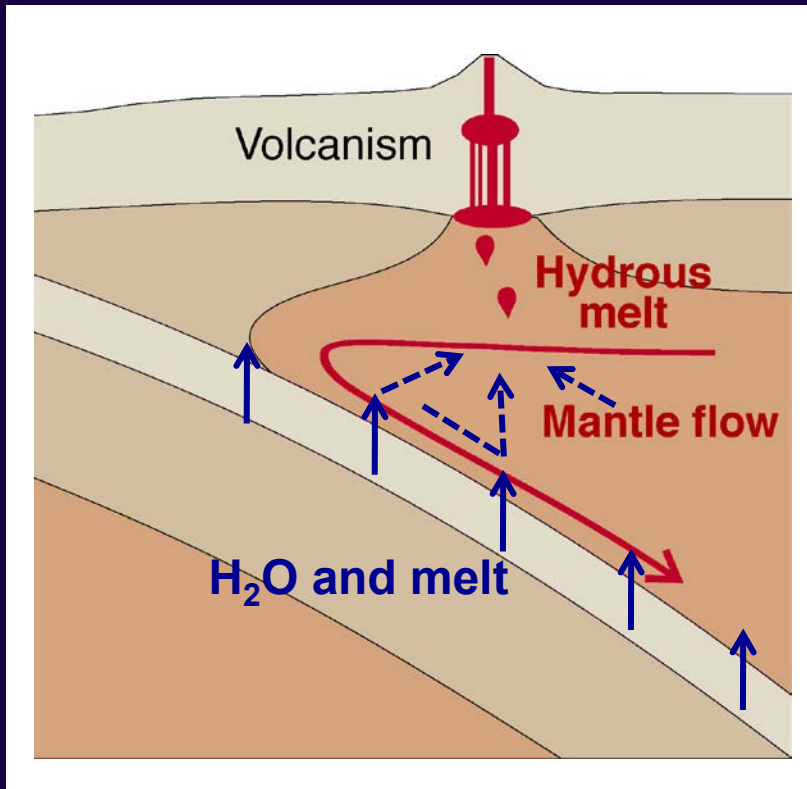
Depleted upper mantle peridotite



"Melange"
50% depleted upper mantle
+ 50% MORB

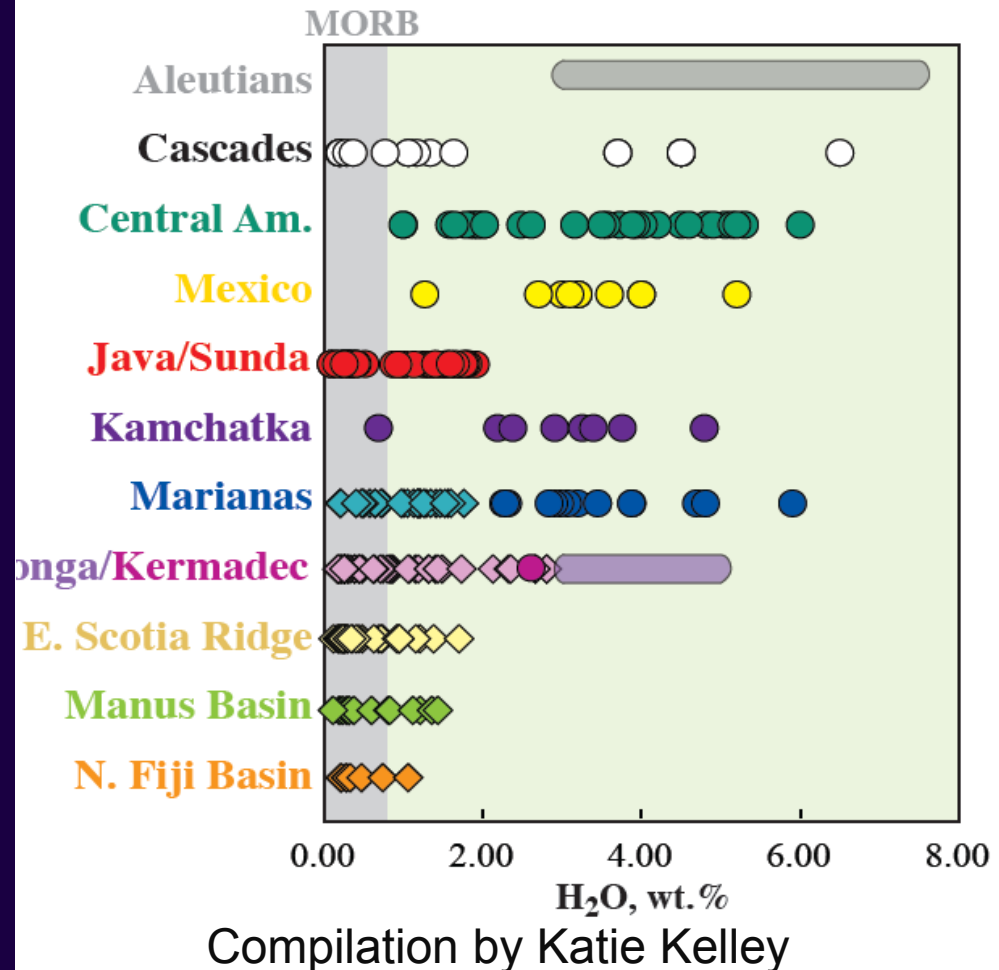


Fluid Migration in the Mantle Wedge



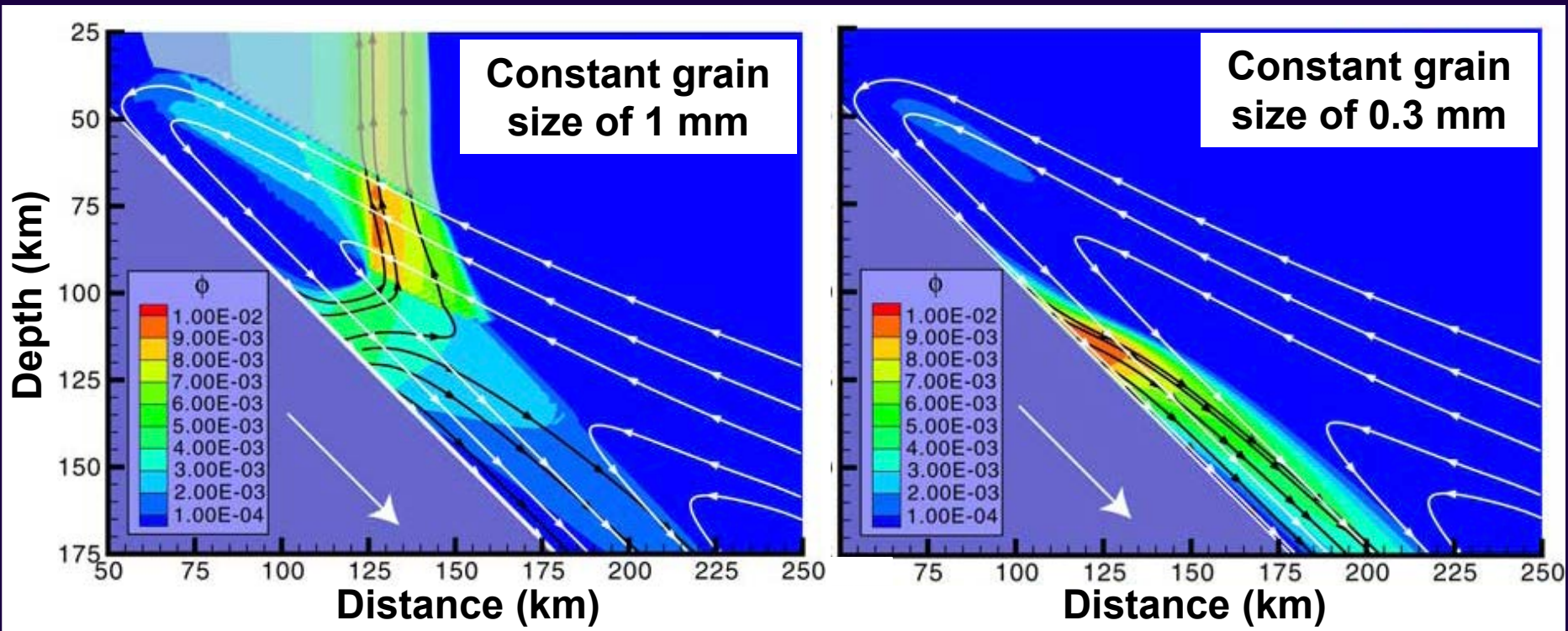
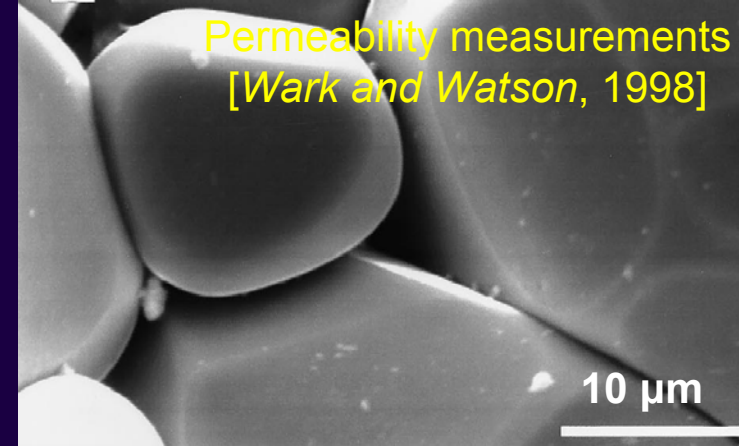
- How does H₂O migrate to the high temperature region?
- Why does the arc tends to form where the slab is 100-120 km deep?

Water in Mafic Arc Magmas (olivine melt inclusions)



- Fluid migration occurs through interconnected pores between grains.
- Grain-scale permeability (k) depends on grain size (d) and fluid fraction (ϕ):

$$k = (d^2 \phi^3) / 270 \quad [Wark \text{ et al.}, 2003]$$

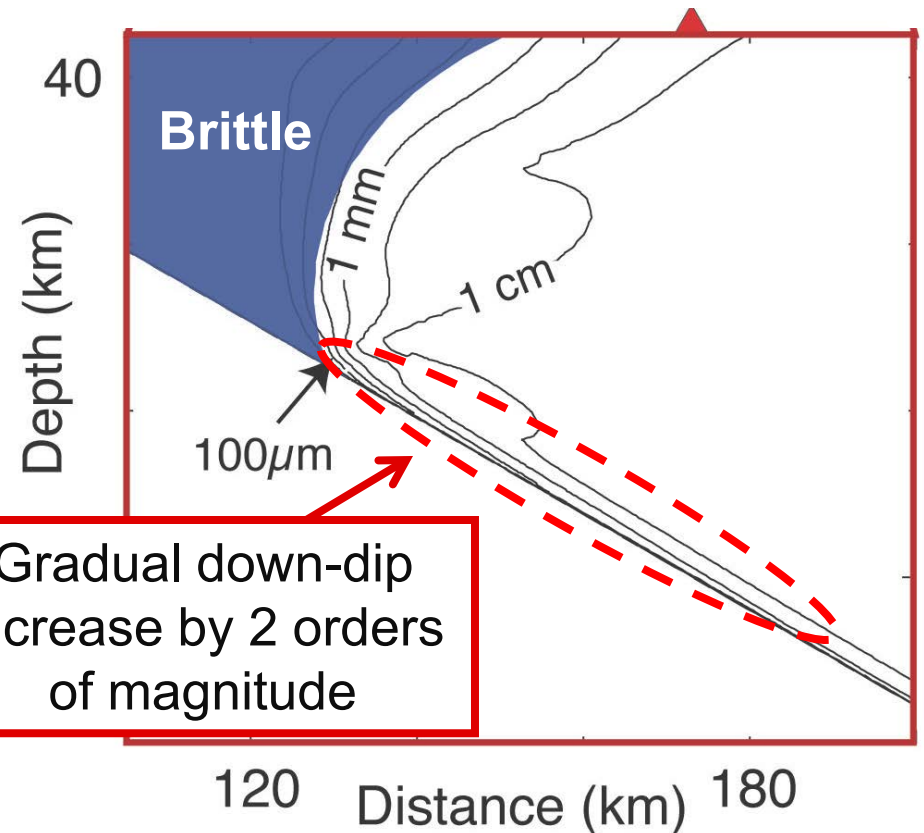
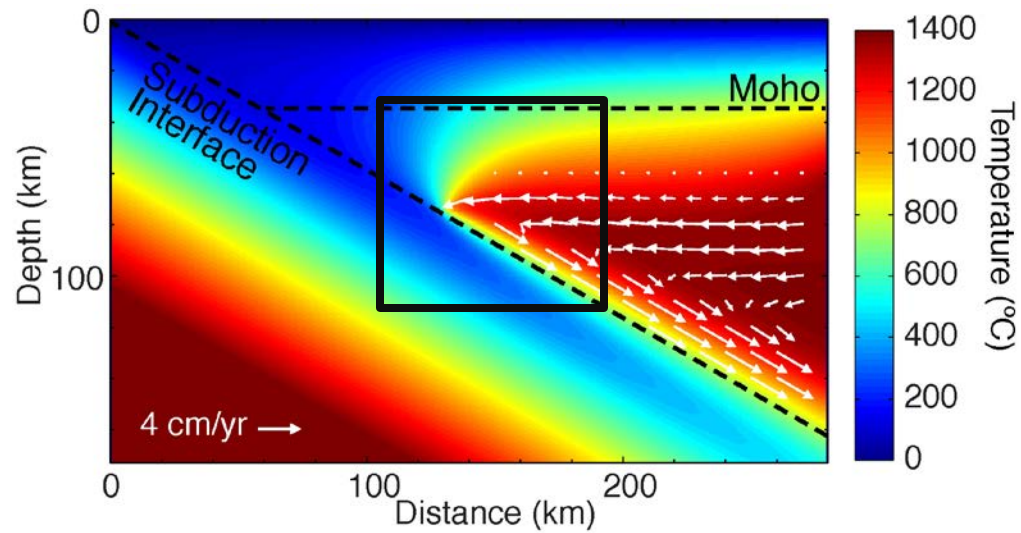


[Cagnioncle et al., 2007]

Steady State Grain Size Distribution

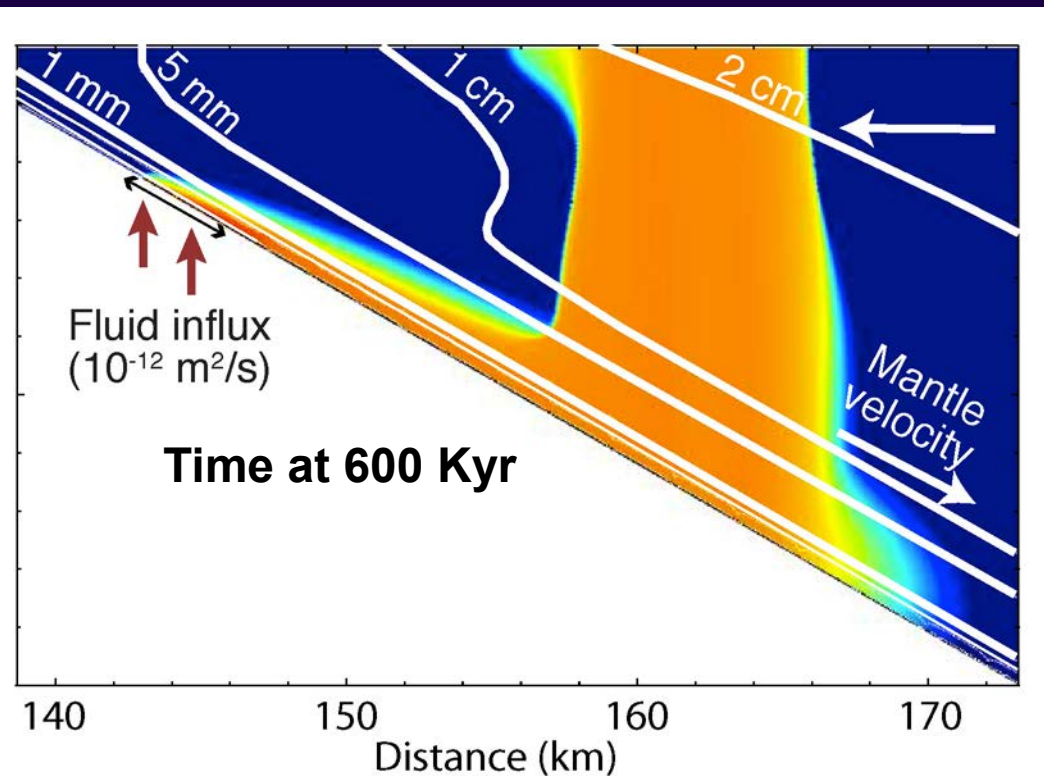
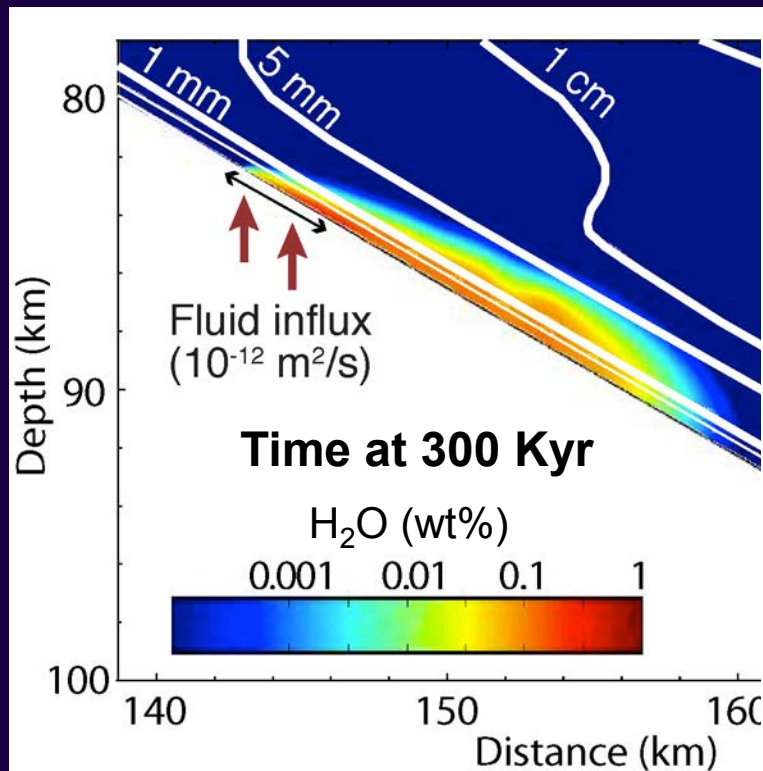
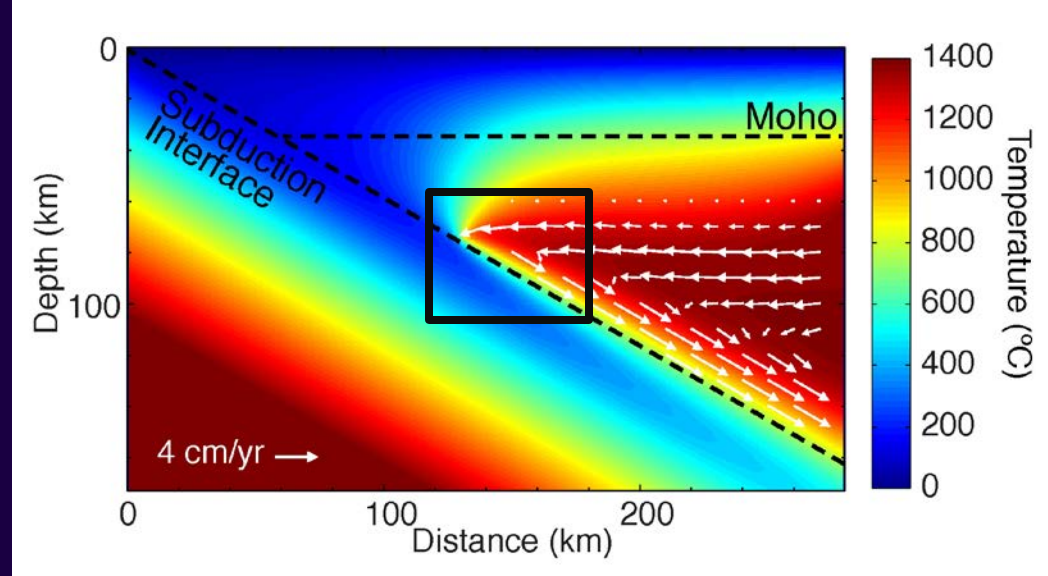
Slab age 100 Ma
Subduction rate 4 cm/yr
Slab dip 30°

Grain size increases
downdip from 10-100 μm to
a few cm, by > 2 orders of
magnitude, independent of
subduction parameters.



Effect of Grain Size Variations

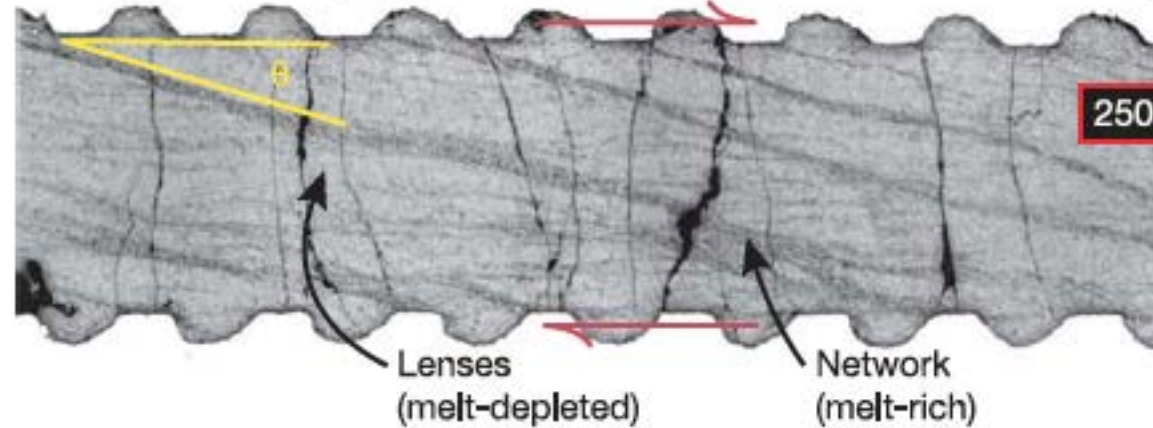
Fluid migration model
in progress



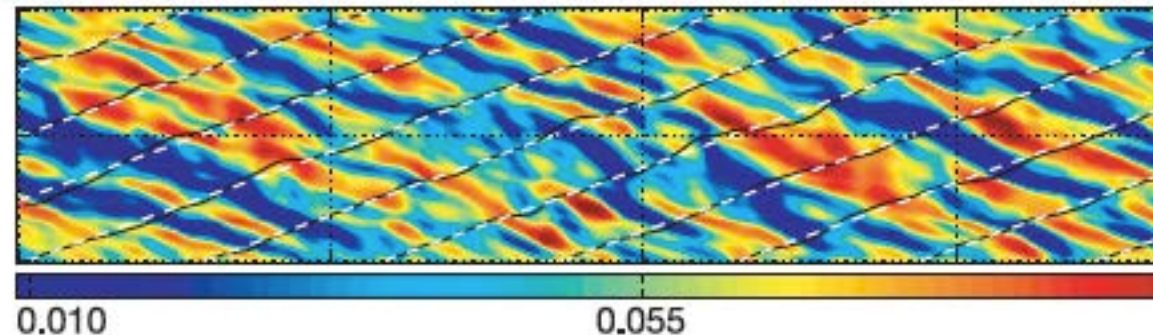
Migration of Aqueous Fluids and Melts

- Plumes/diapirs [*Hall and Kincaid, 2001; Gerya and Yuen, 2003; Currie et al., 2007; Behn et al., 2011*]
- Shear induced melt bands [*Spiegelman, 1993; Katz et al., 2006; Butler, 2009*]
- State of stress in the overlying plate
- ...

a Olivine + chromite (4:1) + 4 vol. % MORB



b Simulated porosity (volume fraction)



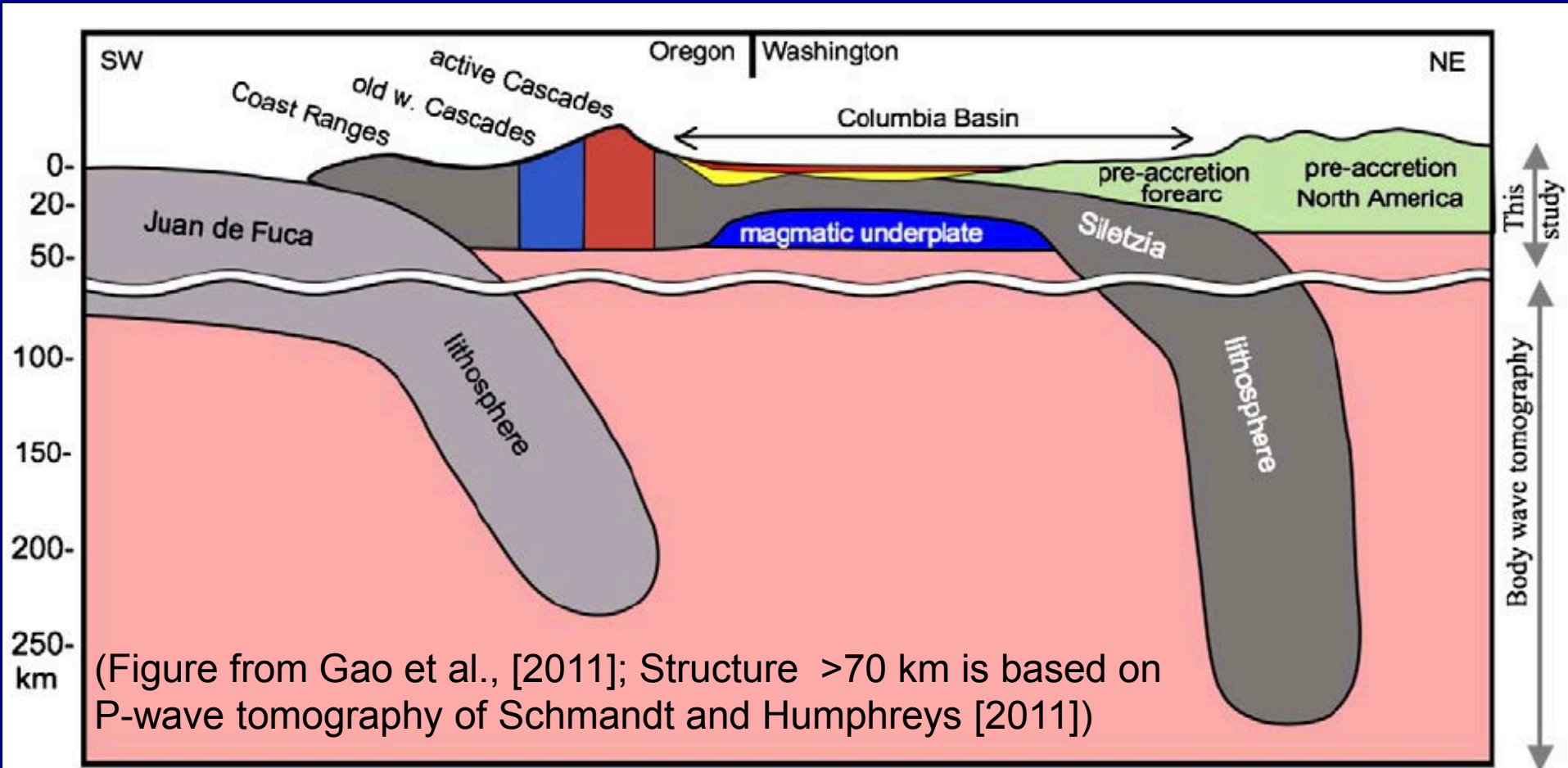
[*Katz et al., 2006*]

Outstanding Questions

- What controls the maximum depth of slab-mantle decoupling – disappearance of mantle-interface strength contrast?
- How does the hot backarc maintained and what is its effect on the arc and forearc region?
- What is the hydration state in the incoming plate and physical properties along deep cutting faults?
- What are the key mechanisms that control the fluid migration path in the subducting slab, in the cold mantle wedge nose, and in the hot flowing mantle?
- What controls the location of the arc?

Competition between slab-driven flow and ...

- Structural obstacles
- “Cold plumes” [Gerya and Yuen, 2003, Gerya et al., 2006]
- Foundering of arc lower crust [Behn et al., 2007]



Seismic Wave Attenuation

Experimentally derived model for shear wave attenuation in melt-free polycrystalline olivine

$$Q_s^{-1}(\omega, T, P, C_{OH}, d) = \left(B d^{-p_q} \omega^{-1} \exp\left(-\frac{(E_q + PV_q)}{RT}\right) \right)^\alpha$$

[Behn et al., 2009, and references therein]

B pre-exponential factor calculated for C_{OH} of 1000 H/10⁶Si

d grain size (1 cm is assumed.)

p_q grain-size exponent

ω Frequency (1 Hz is assumed.)

E_q activation enthalpy

V_q activation volume

α non-dimensional frequency dependence

Grain Size Evolution Model

[Austin and Evans, 2007, 2009; Behn et al., 2009]

Change in grain size = Static grain growth + Dynamic recrystallization (by dislocation creep)

$$\dot{d} = \left[\frac{G_0}{p_g} \exp\left(-\frac{E_g}{RT}\right) d^{1-p_g} \right] + \left[-\frac{\chi \sigma \dot{\epsilon}_{dislocation}}{c\gamma} d^2 \right]$$

(Wet olivine parameterization) Temperature Stress × dislocation-creep strain rate

Note: Two main deformation mechanisms in the upper mantle are dislocation and diffusion creep.

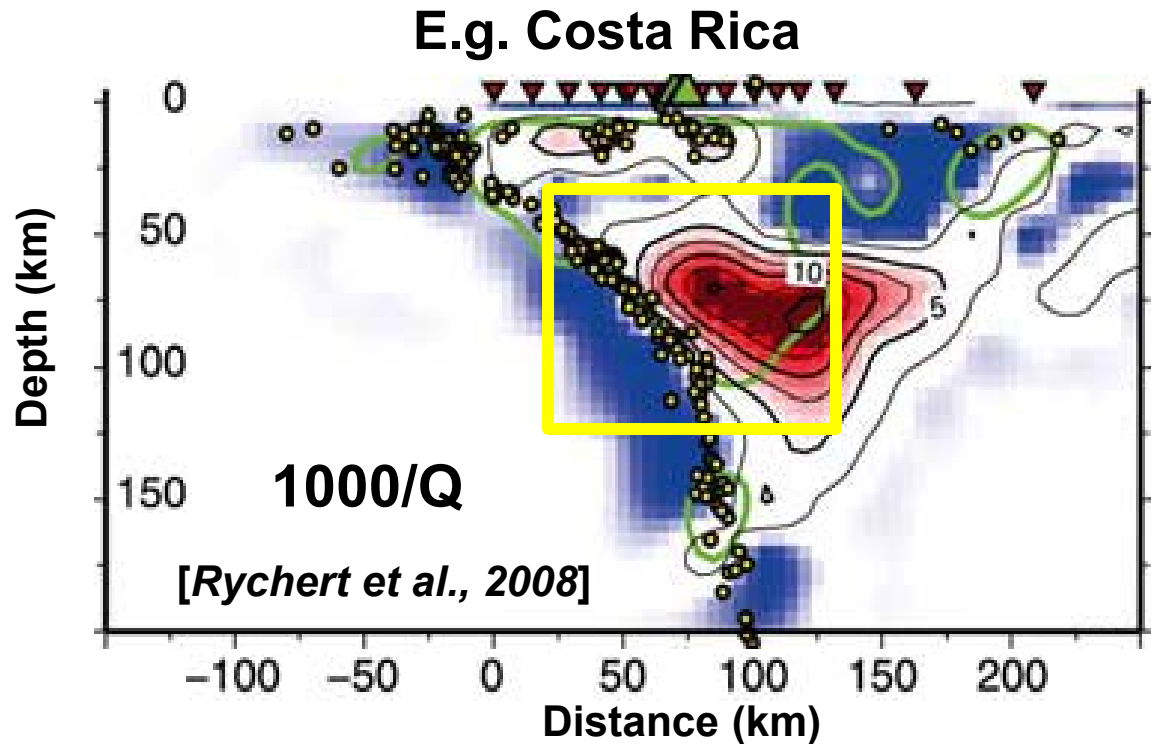
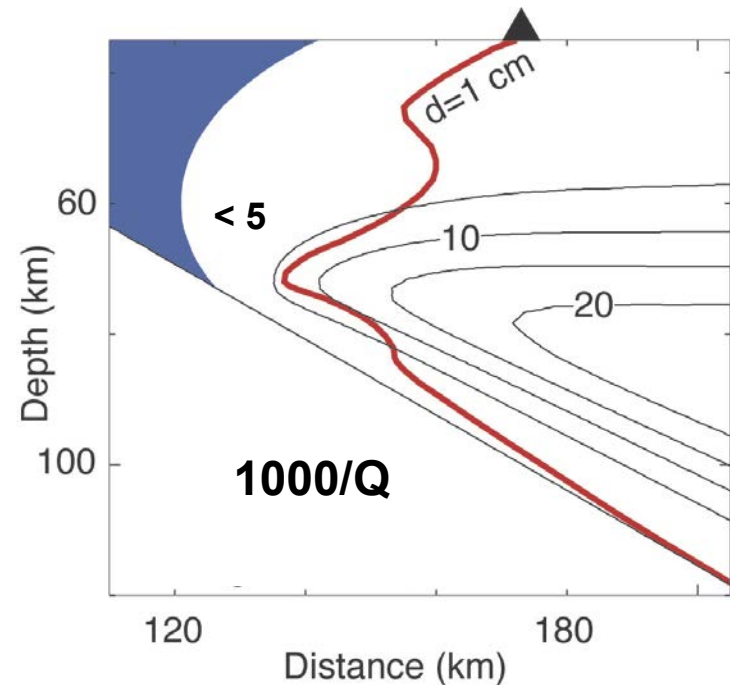
- Grain size reaches equilibrium faster than the rate of change in T and deformation conditions and thus a steady state is assumed.
- The model does not account for brittle deformation and is valid only for creeping regions ($> 600^\circ \text{ C}$).
- Maximum grain growth up to 1-2 cm due to the effect of grain boundary pinning is assumed.

Seismic Attenuation (Q^{-1})

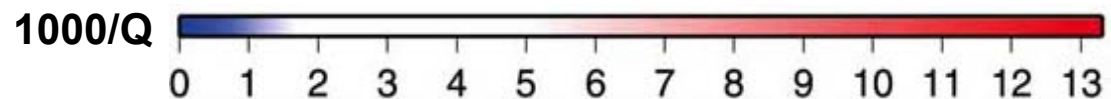
$$Q^{-1} = \left(B' d^{-p} \omega^{-r} \exp\left(-\frac{E_Q}{RT}\right) \right)^\alpha$$

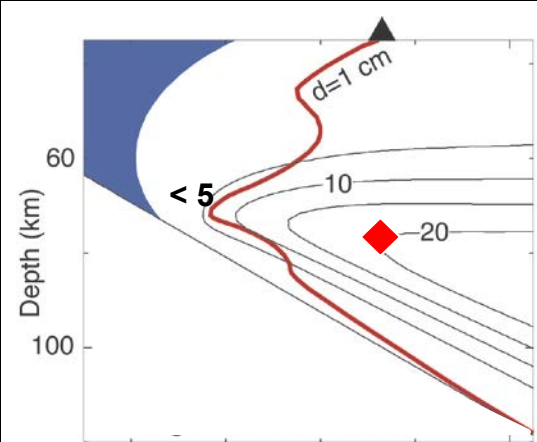
[Behn et al., 2009]

Q^{-1} increases with increasing T and decreasing d .

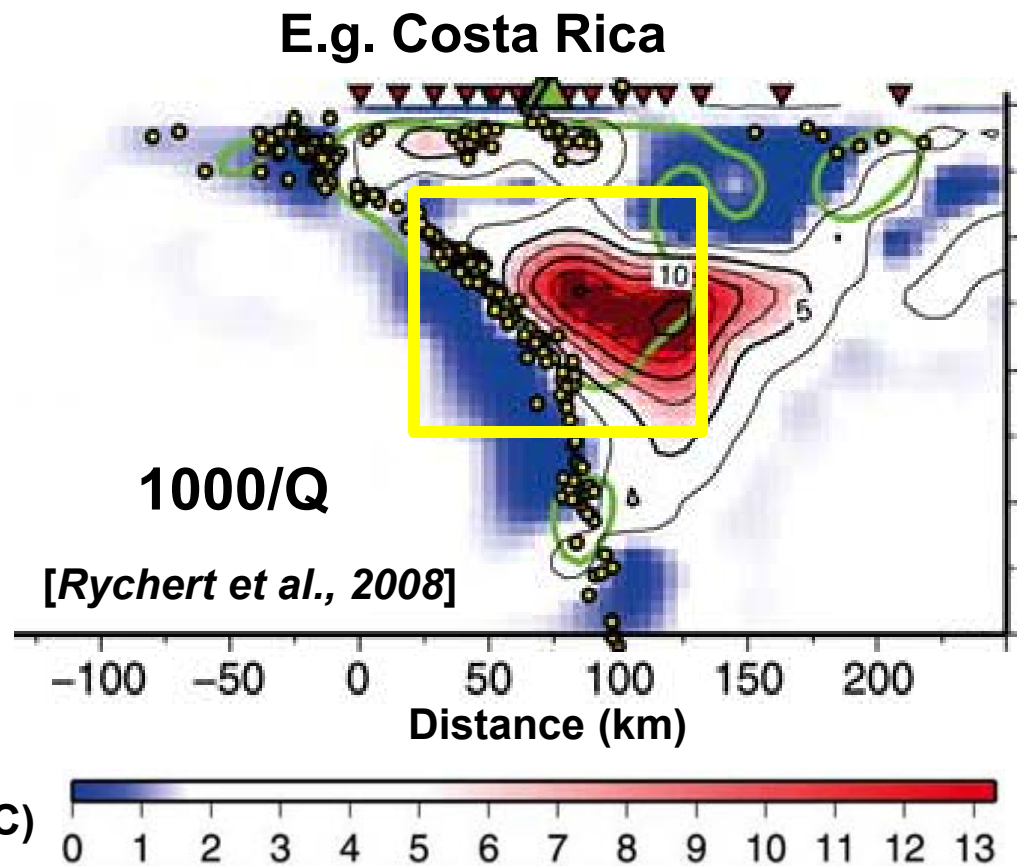
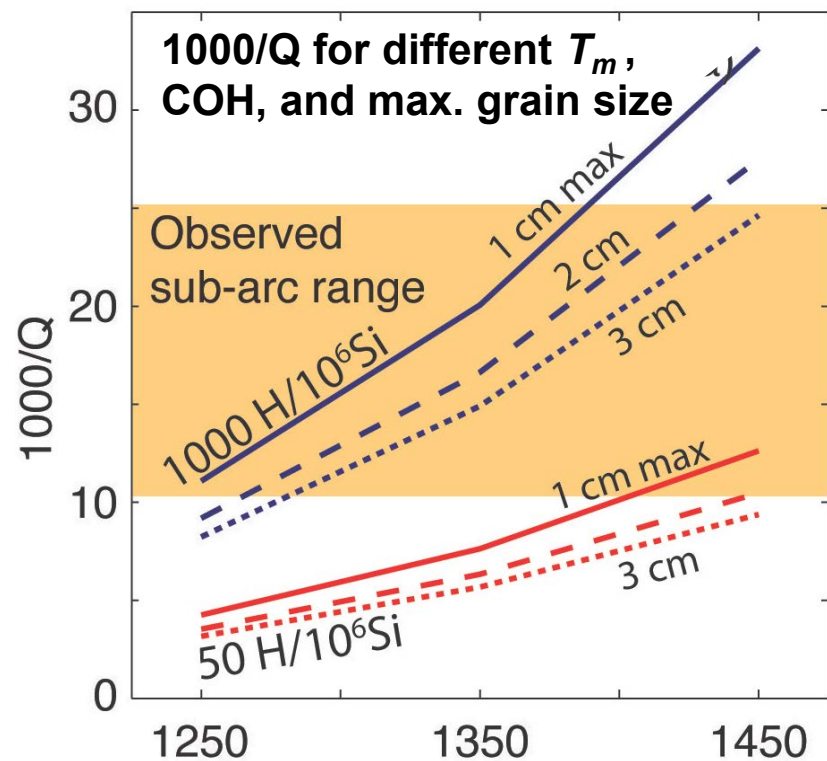


C_{OH} 1000 H/ 10^6 Si
Frequency (ω) 1 Hz



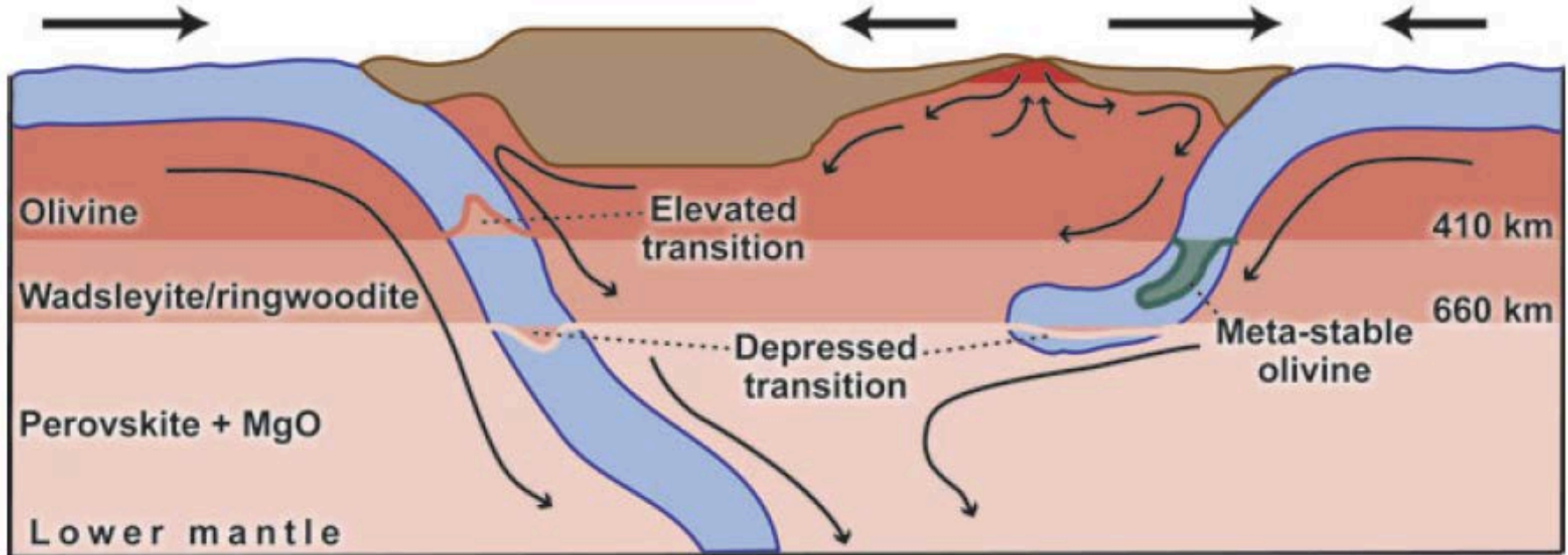


- Predicted attenuation for 1000 H/10⁶ Si beneath the arc is consistent with the observations without invoking the effect of melt.



Back-arc mantle potential temperature (° C)

Slab Dynamics



“Modeling the dynamics of subducting slabs”
by *Billen* [2008, *Annu. Rev. Earth Planet. Sci.*]

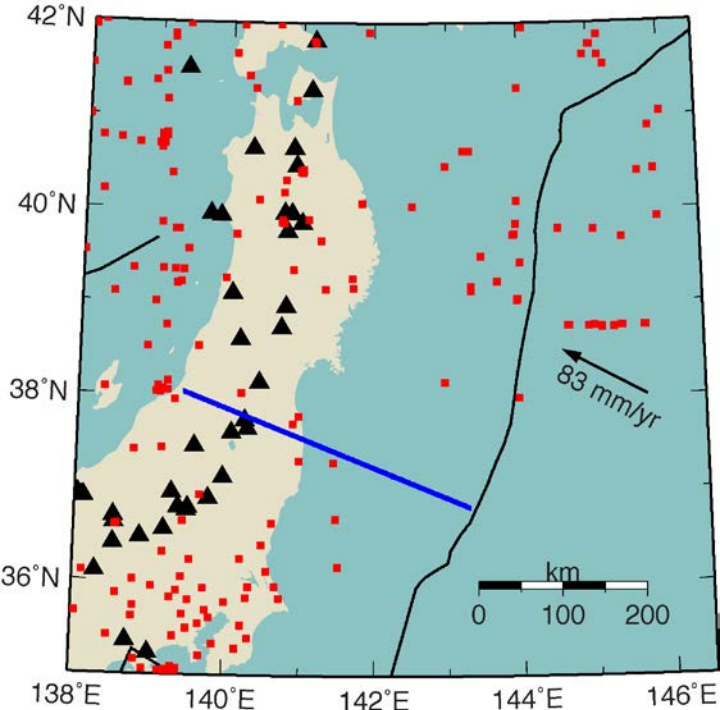
What controls the slab dynamics?

- Buoyancy of the slab
- Rheologies of the slab and the surrounding mantle

Both depend on T , composition, phase transformations, grain size, water content and melt fraction [Billen and Hirth, 2007].

Common Depth of Decoupling

NE Japan

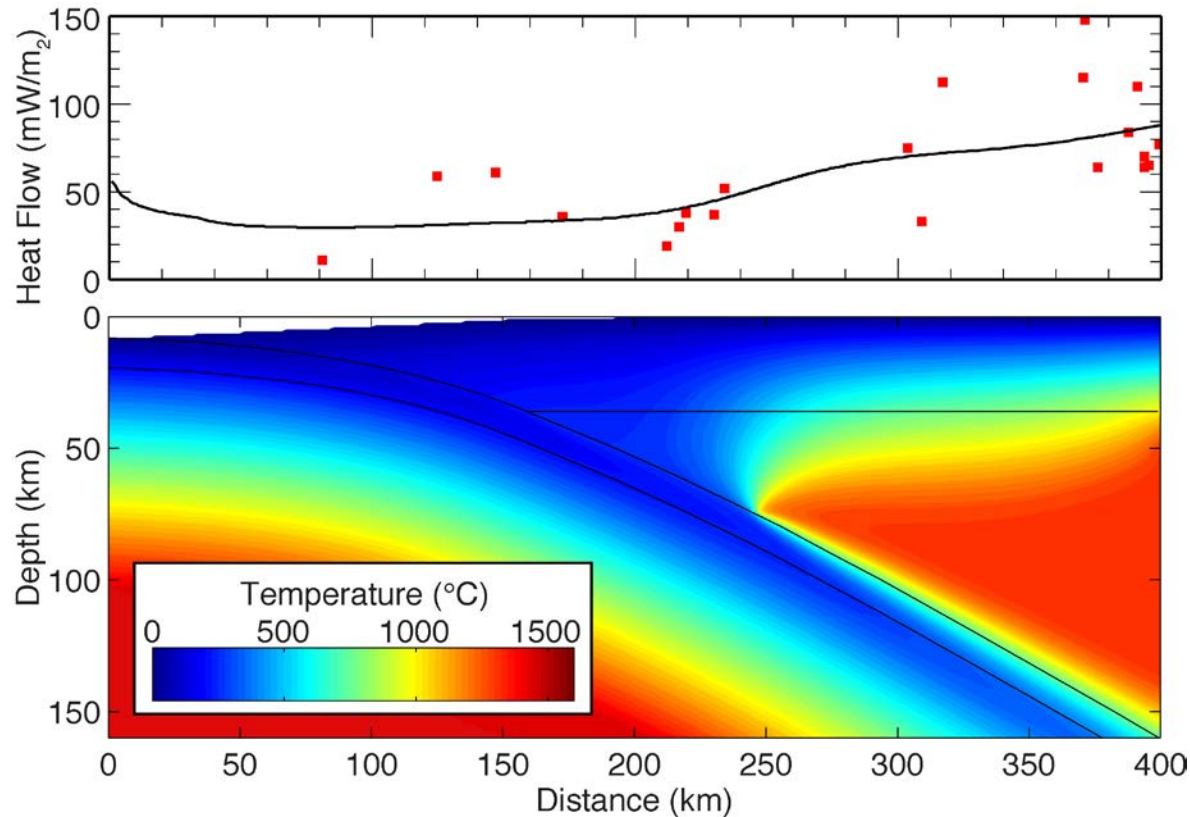


Slab age: 100 Ma

Subduction rate: 83 mm/yr

Frictional heating 0-40 km depths

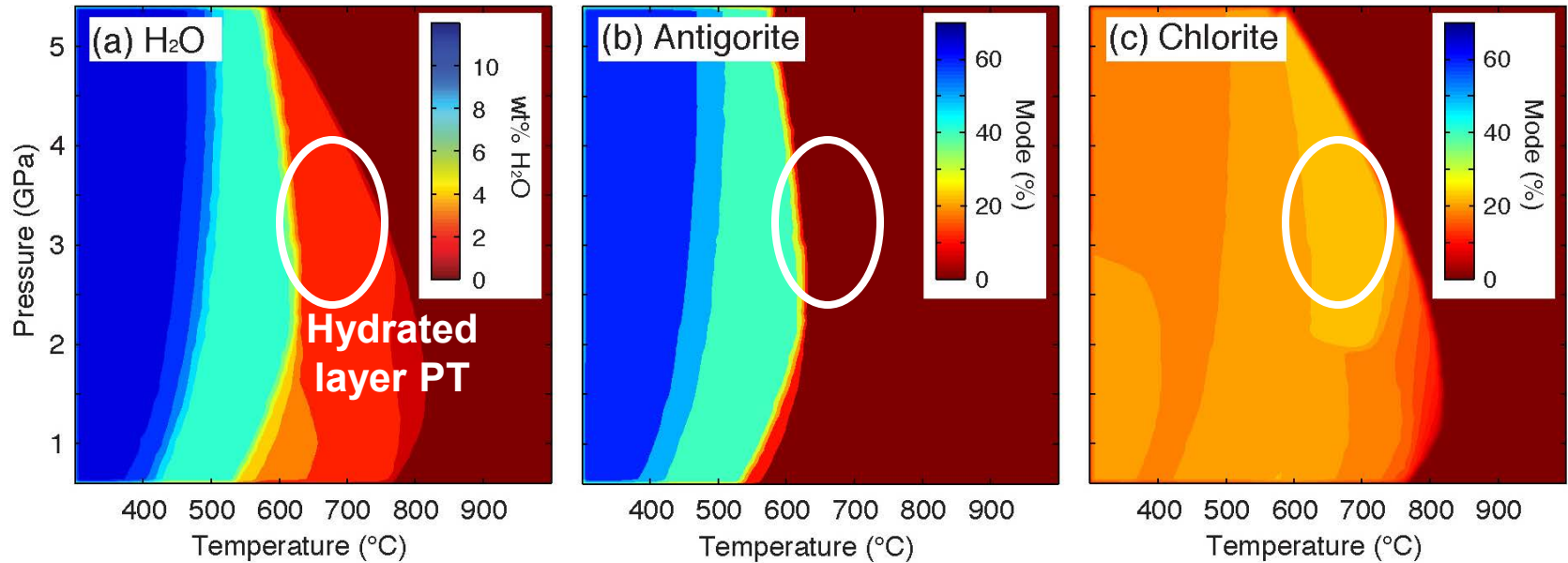
Max. depth of slab-mantle decoupling: 75 km



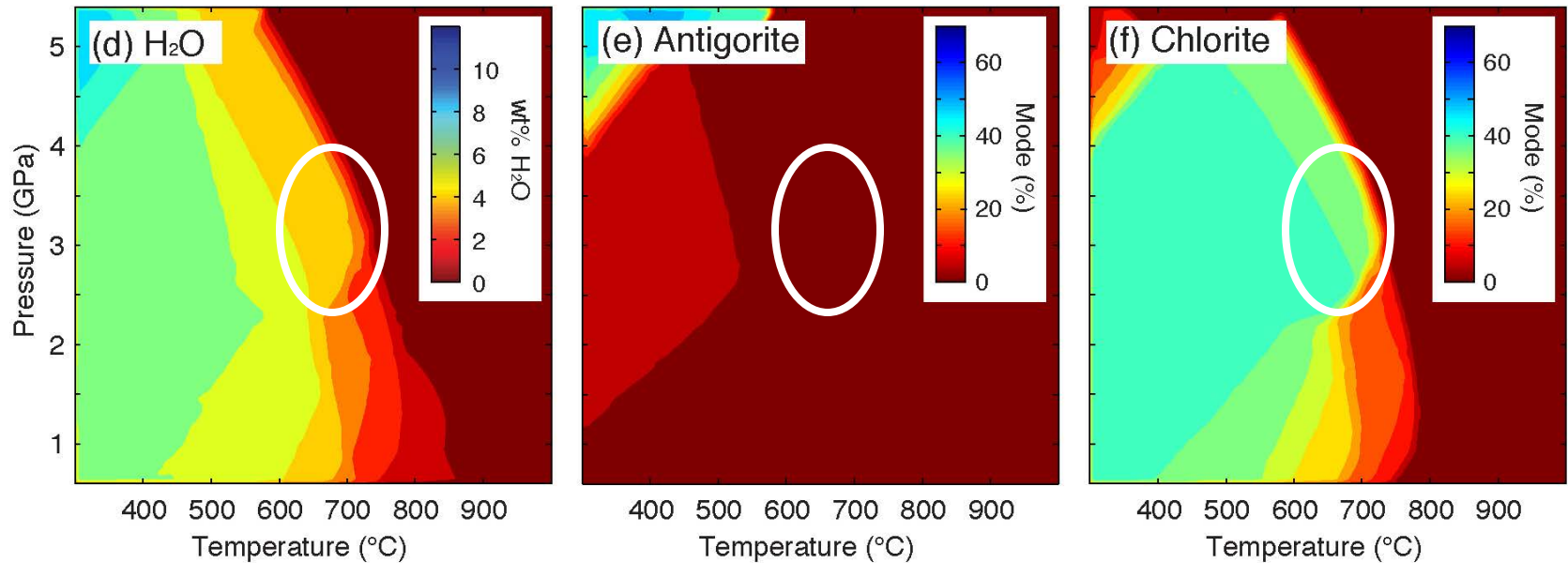
Figures modified from *Wada and Wang [2009]*

- The MDD tends to be 70-80 km [*Wada et al., 2009; Syracuse et al., 2010*]

Depleted upper mantle peridotite at saturation

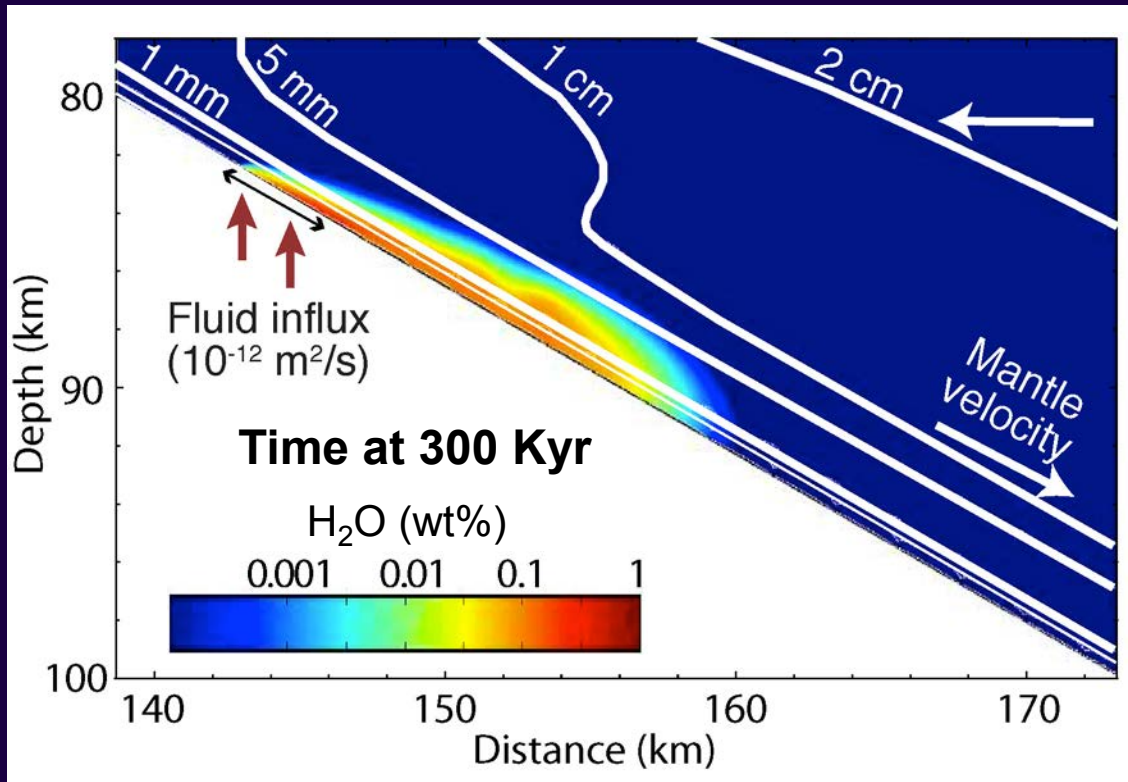
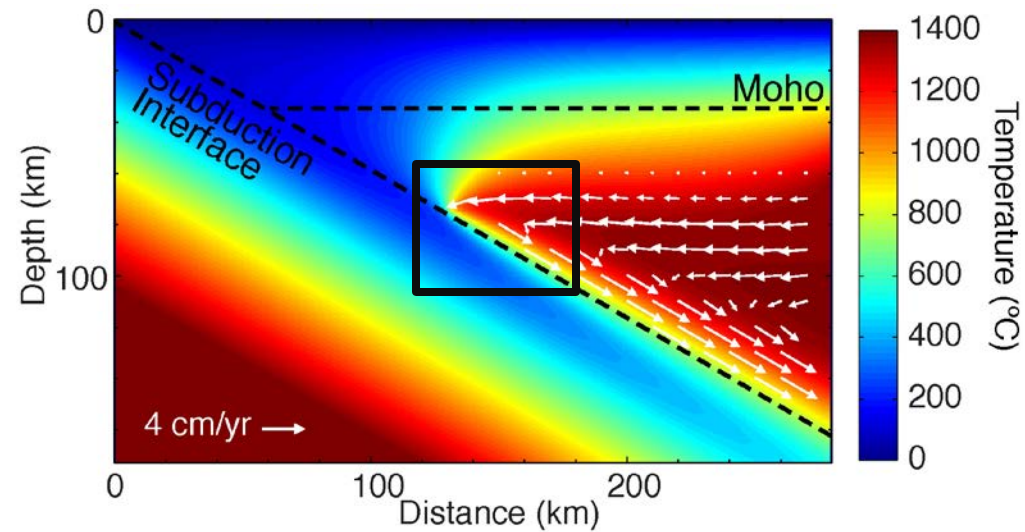


"Melange" (50% depleted upper mantle + 50% MORB at saturation)



Effect of Grain Size Variations

Fluid migration model in progress [I. Wada, M. Behn., and E. M. Parmentier]



Fluid velocity

$$\vec{V}_f = \vec{V}_m + \frac{\vec{S}}{\phi}$$

Darcy's flux

$$\vec{S} = -\frac{k}{\eta} [\Delta\rho\vec{g} + \nabla P]$$

Permeability

$$k = \phi^3 d^2 / 270$$

Conceptual Model for Fluid Migration

